

CRANFIELD UNIVERSITY

NOGARET BAPTISTE

AUTOMATED FOOD LOG ANALYSIS

**SCHOOL OF AEROSPACE, TRANSPORT AND
MANUFACTURING**

Computational and Software Techniques in Engineering

**Master of Science
Academic Year: 2015–2016**

**Supervisor: Dr RÜGER Stefan
August 18, 2016**

CRANFIELD UNIVERSITY

**SCHOOL OF AEROSPACE, TRANSPORT AND
MANUFACTURING**

Computational and Software Techniques in Engineering

Master of Science

Academic Year: 2015–2016

NOGARET BAPTISTE

Automated food log analysis

**Supervisor: Dr RÜGER Stefan
August 18, 2016**

This thesis is submitted in partial fulfilment of the requirements for the degree of Master of Science.

© Cranfield University 2016. All rights reserved. No part of this publication may be reproduced without the written permission of the copyright owner.

Abstract

Automated food log is a promising exemplar of image analysis which allows users to upload their meal pictures that are processed to keep track automatically of one's food intake. It is a challenging problem due to the high variability of dishes (picture conditions, various types, plating).

With this purpose, the presented master thesis describe a process for simultaneous localisation and recognition. To tackle this problem, several feature descriptors and classifiers were sought to obtain the highest efficiency. From the experiments, the leading method is based on two steps. First, a convolutional neural network pre-trained to detect salient objects is applied on each image to generate bounding boxes for every food area and second, an additional convolutional neural network is used in combination of random forest to recognize the food in each bounding box.

Evaluated on the UEC-FOOD 256 dataset, the method enhances the current best segmentation algorithm with 74% of top-1 accuracy. Overall, an accuracy of 28 % is obtained.

Keywords

Food log; Photo; Localisation; Classification; Convolutional neural network, Random Forest

Contents

Abstract	v
Table of Contents	vi
List of Figures	viii
List of Tables	x
List of Abbreviations	xiii
Acknowledgements	xv
1 Introduction	1
2 Previous work	7
2.1 Food localisation	7
2.2 Food recognition	10
2.3 Food log application and intake estimation	15
3 Feature descriptor	25
3.1 Local binary pattern	26
3.2 Colour descriptor	28
3.3 Bag-of-Words	31
4 Machine learning	37
4.1 Decision tree and random forest	37
4.2 Support Vector Machine	39
4.3 Convolutional neural network	42
5 Dataset	45
5.1 Choice of the dataset	45
5.2 UEC FOOD-100 and UEC FOOD-256	46

6 Methodology	49
6.1 Hyperparameter optimization	49
6.2 Localisation	50
6.3 Food recognition	52
6.4 Code	54
7 Evaluation	57
7.1 Environment	57
7.2 Segmentation metrics	58
7.3 Cross validation	59
7.4 Results	60
8 Future work	67
A Appendix	69
A.1 File structure of UEC-FOOD 256	69
A.2 List of food categories (UEC-FOOD 256)	72

List of Figures

1.1	Obesity and overweight rate of the adult population in the uk between 1980 and 2030. <i>Source: World Health Organisation</i>	1
1.2	Average classification and localisation error of the best results for different ImageNet challenges	3
1.3	Examples of high intra-class variability for kaya toast	5
1.4	Examples of low inter-class variability for kaya toast	5
2.1	USDA MyPyramid original logo	16
2.2	Annotated screenshot of the FoodCam application	22
3.1	Illustration of the LBP descriptor's process	27
3.2	Pyramid representation of the HSV channels	29
3.3	Illustration of the Bag-Of-Visual-Words model	32
3.4	Illustration of the difference of Gaussian over multiple octave	33
3.5	Illustration of SIFT as a local image descriptor	34
4.1	Decision tree of for ten elements belonging to two classes	38
4.2	A regular 3-layer neural network	42
4.3	Example of a 16-layer deep convolutional neural network	43
4.4	Illustration of a max pooling layer of stride 2	44
5.1	Pictures with multiple food items from UEC FOOD 256	48
6.1	General process of the localisation and classification	50
6.2	Picture of the 100 possible bounding boxes that the salient CNN will try to recognise	51
6.3	Segmentation result	53
7.1	Illustration of 4-fold cross validation	59
7.2	Curves of Accuracy over IoU (top), Precision over IoU (centre) and Recall over IoU (bottom)	61
7.3	Classes having the highest accuracy	63
7.4	Classes having the lowest accuracy	63
7.5	Most confused classes	64

A.1	UEC-FOOD 256 list of files and directory in the root	69
A.2	UEC-FOOD 256 file: <i>category.txt</i>	70
A.3	UEC-FOOD 256 file: <i>multiple_food.txt</i>	70
A.4	UEC-FOOD 256 file: <i>bb_info.txt</i>	71

List of Tables

5.1	Summary of some available food datasets according to the criteria	46
7.1	Average localisation accuracy result for UEC FOOD 256	60
7.2	Average classification accuracy result for UEC FOOD 256	62
7.3	Average accuracy result for simultaneous localisation and recognition on UEC-FOOD 256	62
7.4	Average accuracy result for UEC FOOD 100	65
A.1	List of all the food categories of UEC-FOOD 256 with the number of pictures associated	83

List of Abbreviations

BoW	Bag of Words
CNN	Convolutional Neural Network
DCNN	Deep Convolutional Neural Network
IoU	Intersection over Union
LBP	Local Binary Pattern
RF	Random Forest
SIFT	Scale-Invariant Feature Transform
SURF	Speeded Up Robust Features
SVM	Support Vector Machine

Acknowledgements

I am really grateful to Dr. Stefan Rüger, my supervisor for the project, to have proposed this subject. His guidance and valuable advice were particularly helpful to realise the thesis.

Moreover, I would like to thank the University of Technology of Compiègne for giving me the opportunity to study one year in Cranfield University. I would also like to thank Cranfield University for its facilities and this great year of study.

I would like to express my gratitude to M. Kazu Shimoda and Pr. Keiji Yanai from the University of Tokyo that made their datasets available and provided enlightenments and further details on their work.

Chapter 1

Introduction

Over the last few decades, the rate of obesity and overweight people in the World has greatly increased. As presented for the UK case in the Fig. 1.1, the obesity rate has increased by 12% between 1980 and 2013, and the overweight rate by 13%. It is forecast by the World Health Organisation to continue to grow in the next decades.

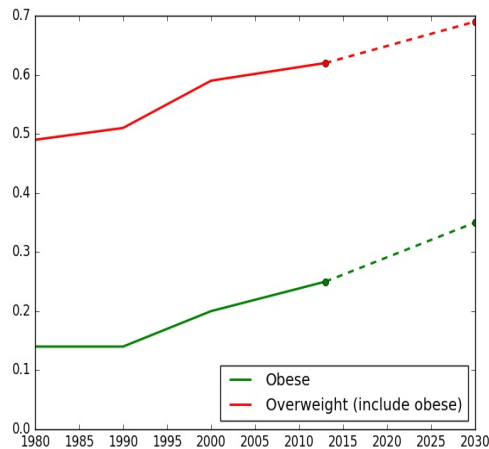


Figure 1.1: Obesity and overweight rate of the adult population in the uk between 1980 and 2030

Being “overweight” is defined as having a Body Mass Index (BMI) – a person’s weight

in kilograms divided by the square of his height in meters (kg/m^2) – of between 25 and 29.9, and “obese” by a BMI of 30 and above.

As stated in [1], obesity is strongly associated with several major health risk factors such as stroke, high blood pressure, type 2 diabetes and high cholesterol. Thus, it has a great human and economic (Zhang et al. [2] in 2010 showed 12% of the total worldwide health expenditure is spent on diabetes and the total cost will continue to grow) cost for societies.

Associated with lifestyle changes, recording what we eat is one way to control our eating. Studies such as [3] show the benefit of reporting its daily diet to lose weight and improve the quality of its food intake. And more generally, it can be a way to treat eat disorders

Yet, manually recording detailed information regarding all meals is a tedious and time consuming task and it is hard for people to adhere to this process for a long time. Moreover, it often needs a trained patient. As presented in [4], user logs are prone to errors (users tend to underestimate its intake).

At the same time, image processing methods has greatly improved the recognition rate of elements in a picture. ImageNet is a dataset containing more than 1,2 million images split into 1000 classes. Since 2010, the yearly challenges include localisation, classification and detection. Numerous researchers, students, educators or information technology companies are participated.

As described in Fig. 1.2 and using data from the challenge result report [5], the mean classification error for each class and localisation has been greatly reduced between 2010 and 2014.

With the widespread use of smartphone, cameras or wearable devices, people can easily take pictures of a good quality and are already taking photos of their food and posting them on website such as Food Gawker, Instagram, Flickr or Yelp.

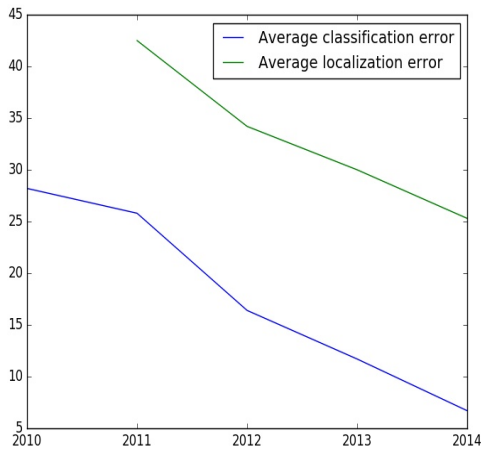


Figure 1.2: Average classification and localisation error of the best results for different ImageNet challenges

That's why, it has recently been proposed to automate the process and assist patient and their medical personnel (nutritionists, psychologists) to understand the patient's behaviour and habits. It extends the reach of care in a cost effective ways and counters some of the previous problem of manual report. It's part of the rise of e-healthcare / m-healthcare [6, 7].

The idea is to have users who upload pictures of their daily meals to the application or website that constructs their food diary automatically. Using image processing, it estimates the dietary composition of the meal and keep record of the information for later viewing in formats such as tables or graphical representations.

Food recognition is a promising applications of image processing and machine learning. Its overall process is:

- Extract key characteristics
- Localise food items if the application allow multiple food items
- Recognise the food

Feature description is essential to achieve good object detection and image categorisation. Preferably the method should be invariant of the conditions, i.e. the luminosity, orientation or scale of the picture.

In this thesis, we focus on the food recognition. It has already numerous challenges such as:

- **high intra-class variability** : we can have high variability between pictures for the same particular kind of food items, due to:

- environmental conditions (e.g. luminosity, quality of the camera)
- plating (the way it is served)
- variation of the way the picture is taken: numerous transformation can be applied to a same picture (scale, translation, rotation, skewness, crop)

This is illustrated in Fig. 1.3 for pictures of kaya toast.

- **low inter-class variability** : we can have low variability between different type of food such as between clear and miso soup as showed in Fig. 1.4.

This makes localisation, classification and retrieval of food images a difficult task for current state-of-the-art techniques, and hence a compelling challenge for image processing and machine learning researchers.

Thus, the thesis is dedicated to the investigation on some methods that were found in the literature. Many modi operandi exist and we focus on three different descriptors: colour and texture features, local feature using Bag-Of-Word representation and convolutional neural network. These methods are evaluated on UEC-FOOD 256 and compared to previous papers. The generation of this dataset was presented by [8] by Kawano et al. from the University of Tokyo in 2015.



Figure 1.3: Examples of high intra-class variability for kaya toast. Pictures extracted from the UEC FOOD 256 dataset [8].



Figure 1.4: Examples of low inter-class variability for clear soup (left) and miso soup (right). Pictures extracted from the UEC FOOD 256 dataset [8].

The organization of this thesis is as follow. In section 2, previous work on food localisation, recognition and intake estimation is reviewed. Section 3 introduces the different image descriptors used, and in section 4 the classifiers are presented. In section 5, the dataset is introduced. Section 7 reports the experimental settings and results. Finally, in section 8, we draw the conclusion and state the limitation and possible future work.

Chapter 2

Previous work

A profusion of techniques have been employed in the literature for food recognition. Yet, localisation and classification have been rarely used simultaneous. That is why these two subjects are presented separately (section 2.1 is dedicated to food localisation, section 2.2 to recognition). Then, some food applications are presented.

2.1 Food localisation

A way to localize food is based on edge detection and colour segmentation.

In [9], Thendral et al. describes and compare these two methods to localise an orange in a picture. It applied these methods on a small dataset of 20 orange images (only one orange per image), with different lighting conditions and backgrounds (pictures are taken from the Internet). In more details, the edge-based segmentation apply the canny-edge segmentation, then apply non-maximum suppression to eliminate noises. Then, each pixels are classified. The colour-based segmentation normalised the lightning condition with a Gaussian low-pass filter, convert the RGB image into a $L * a * b$

1. Gaussian low pass filter to normalize the lightning condition

2. convert the image from RGB representation to $L * a * b$
3. use the a channel to classify each pixel as “fruit” or “non-fruit”
4. remove small object
5. fill the binary image regions and holes

For orange detection, the colour segmentation has an higher accuracy. Yet, it is very hard to generalise this method as it has only been tested on oranges, a food item with a very distinctive colour.

An other method for food detection relies on circle detection. Indeed, food items are often served in a round shape container such as a bowl, pan or plate.

In [10], Wazumi et al. describe their use of the Hough transformation. The purpose of this technique is to find approximations of instances a certain class of shapes by a voting procedure. In this paper it is used to detect circles assuming the food is only contained in round plates or bowls and with edges not obstructed on the picture (it performs poorly with cropped pictures). Keeping only the central part of the circle, the segmentation is then fed to the recognition process.

A more recent development is the used of convolutional neural network.

In [11], Shimoda et al. presents their segmentation process based on a pre-trained deep CNN.

The proposed pipeline is composed of 6 main steps:

1. detect all the possible bounding box (maximum 2000 per image) using selective search
2. cluster the bounding box, using the ration of intersection over union (IOU, also call overlap ratio) to obtain 20 at most.

3. a Deep CNN for all the selected bounding box to get a saliency map. The DCNN is modelled on AlexNet CNN, was pre-trained on the Salient Object Subitizing (14 000 everyday pictures) dataset and fine-tuned on UEC FOOD 100.
4. use the GrabCut algorithm to extract the foreground region from the food area. GrabCut is an iterative method using graph cuts to extract foreground from background based on an initial guess.
5. In case of overlapped bounding box, the authors proposed to apply the non-maximum suppression (NMS) algorithm.

The authors apply this process on the UEC-FOOD 100 dataset and PASCAL VOC 2007. The latter is used for object detection and recognition of 20 common classes (train, tv, cat, human ...)). These two datasets use bounding box to spot items. A segmentation is correct if the overlap ratio exceeds 50% between the predicted and the ground truth bounding box.

UEC FOOD 100¹ is a dataset created by Matsuda et al. in [12] containing 100 types of food, mainly Japanese food, and is composed of 9060 pictures. Thus, an image can contain multiple dishes. That's why each food picture is associated with the bounding box coordinates indicating the food localisation.

For UEC-FOOD 100, the authors obtain 49.9% mean average accuracy and 58.7% for PASCAL VOC 2007.

A pre-trained DCNN is also used by Bolanos et al. [13] to classify each pixel as food or non-food. The DCNN is modelled on “GoogleNet” [14], a neural network composed of 22 layers and first used on ILSVRC14 (ImageNet Large Scale Visual Recognition Competition 2014). On UEC-FOOD 256, the authors obtain 60% of accuracy.

¹Dataset can be found at <http://foodcam.mobi/dataset100.html>

UEC FOOD 256² is presented in [8] and it is an extension of UEC-FOOD 100 (same creators' team). It adds 156 kinds of food from all over the world (French, Italian, Vietnamese, American, ...). As for UEC-FOOD 100, every food photo has a bounding box indicating the food location.

2.2 Food recognition

Over the last few years, authors have focused on food recognition. Various methods were tried. For feature extraction, it often combines colour and texture descriptors, global and local.

In [15], Chen et al. create a new dataset named PFID and provide two simple food classification baseline methods. PFID (stands for Pittsburgh fast-food image dataset)³ was presented in [15] in summer 2008 from the collaboration of Intel Labs Pittsburgh, Columbia and Carnegie Mellon universities. It is one of the first mature datasets released for food recognition.

It contains 101 meals (categories) from 11 popular fast food chains found in the USA with images and videos captured in both restaurant conditions and controlled lab setting. It contains foods such as chickens, sandwiches, salads, burgers and drinks from Arby's, Bruggers Bagels, Dunkin Donuts, KFC, McDonalds, Panera, Pizza hut, Quiznos, Subway, Taco Bell and Wendy's.

In their paper, Chen et al. provide two baseline methods:

- Colour histogram and SVM classifier. They obtain a mean accuracy of around 12%.
- Bag-of-Features using SIFT and SVM classifier. They obtain a mean accuracy of around 25%.

²Dataset can be found at <http://foodcam.mobi/dataset256.html>

³Dataset can be found at <http://pfid.rit.albany.edu/>

Song et al. [16] use also a Bag-of-Word method using SIFT for detection of the keypoints and LBP for description. They use a local texture feature and their spatial distribution to classify food images from the PFID. The shape context algorithm is used to keep the spatial relationship between codewords (for each image, compute the histogram of one word compared to the others / then mean of the histograms).

For the classification, the authors pick the smallest cost between an image and a food category. For each interest points found with SIFT in the image, we associate a similarity between the point and each visual words of the codebook. The similarity function is based on the Bhattacharyya distance. Then, the shape context between the point of interests and the visual word is calculated and a cost is deduced for each food category. The category with the smallest cost is chosen.

Regrouping the different pictures in 6 main groups the PFI dataset (sandwiches and wraps, meat, salads, donuts, hamburger and miscellaneous), they obtain an average accuracy of 66%.

Moreover, Fast foods, as they are standardized and have nutrition information available online, can easily be used to measure the calories. In [17], the authors are using the PFID's videos to estimate energy intake of a meal.

While Chen et al. use global and local features separately, Bosch et al. [18] combine to identify the food consumed. For the global features, they use colour properties (entropy, histogram and moments) with texture information provided by Gabor filters. They add local features with the Bag-Of-Features, using SIFT for detection and SIFT, steerable filters and DAISY descriptors. To classify, they use SVM (using the Radial Basis function kernel). On a in-house dataset composed of 28 classes and 179 images, the authors obtain 86% of accuracy.

Still evaluated on PFID, Yang et al. [19] use a novel feature, named PFD (for pairwise local feature distribution) for food recognition.

The different steps of this method are:

1. classify each pixel in one of the categories between beef, chicken, pork, bread, vegetable, tomato/tomato sauce, cheese/butter, egg/other and background. For classification, they use the Semantic Texton Forest, method based on local characteristics. It was previously trained on 16 manually-labelled pictures.
2. Global ingredient representation (GIR): for the 8 food categories, it sum up the soft label of all the ingredient pixel and normalize by the number.
3. PFD: geometric pairwise feature on N ingredient pixels (picked randomly, thus $N / 2$ pairs):
 - log of the distance
 - orientation
 - soft label of the midpoint
 - soft label of each pixel along the line connecting the pair of pixels
 - joint feature (a mixed of the above characteristics)

Accumulate the pairwise values into a distribution (using a multi-dimensional histogram of either 8 or 12 bins), weighted by the soft labels of the two pixels. Each pixel is mapped to its closest bin in the histogram. Then, normalization of the histogram.

Fed to a linear SVM, they obtain an accuracy between 19% and 28% for each of the 61 categories. When they pick the 6 major types of food, they get almost 80% of accuracy.

In [20], the author use the Random forest clustering algorithm to create superpixels (selecting only the discriminative one). On these superpixels, a dense SURF and L*a*b* color value is computed and encoded with improved fisher vectors (IFV) with

Gaussian mixture model (GMM) of 64 Gaussians. Then, they use PCA to reduce the size of the vector and the machine learning method is structured-output multi-class SVM. They use their method on their new dataset named ETHZ Food-101 (56% accuracy) and MIT-indoor (58% of accuracy on the full dataset) and compare it against several previous implementations.

ETHZ Food-101⁴ is composed of 101 categories, 1000 images per category (250 pictures manually reviewed, used for the test set and 750 with noises for the training test). Pictures were extracted from the website foodspotting.com. The top 101 most popular dishes from this social sharing food images defined the categories.

[21] present a method to automatically identify food and estimate the quantity. It is used on an in-house dataset composed of 50 categories, mainly Chinese fishes, with 100 pictures per class. For recognition, the authors use:

- local information with Bag-Of-Words, using SIFT as descriptor and Local binary pattern on a 3-level pyramid
- global information: colour histograms and Gabor filters extracted from each block (image divided into 4×4 blocks)

They train a SVM classifier for each category, then fuse them with the multi-class AdaBoost algorithm. AdaBoost, or “Adaptive boosting” is a meta-algorithm that combine into a weighted sum multiple classifiers to improve their final performance. The authors get an overall accuracy of 68.3%. If we keep the top-3 results, the accuracy is even 90.9%.

More recently, people have started to heavily use Convolutional Neural Networks CNN with great results.

In [22], the authors created a new dataset named UMPc Food-101 (“twin dataset” of ETHZ Food 101) combining text and visual information for recipes. As a proof of

⁴Dataset can be found at https://www.vision.ee.ethz.ch/datasets_extra/food-101/

concept, they develop a search application for recipe recognition. The user send a query (a food image) and as a result, the three best recipes (categories) are displayed.

UMPC Food-101⁵ is a “twin-dataset” of ETHZ Food 101 as it is composed of the same 101 categories, with 1000 images per category. Yet, the pictures have been crawled from Google image, researching for recipes. Thus, most images are associated with a text.

For the image recognition model, they use textual, visual or a mix of both features:

- visual feature (all feeding a SVM):
 - Bag-of-Words using a dense SIFT and a codebook of size 1024 on a 3-level spatial pyramid. They obtain an average accuracy of 23.96%.
 - Use an improved version of the Bag-of-Words named “BossaNova”. It modifies the pooling system; instead of keeping the closest cluster of a SIFT descriptor, it represents it by keeping distances between the descriptor and all the codebook words. Average accuracy of 28.59%.
 - Use a deep CNN as a feature descriptor, using the 7th layer of a pre-trained CNN ("OverFeat"). Average accuracy of 33.91%.
 - Use a very deep CNN as a feature descriptor, using th 19th layers ("vgg-verydeep-19"). Average accuracy of 40.21%.
- text-feature: use the term frequency - inverse document frequency *tf-idf* method and get 82.06% accuracy
- fusion of textual and visual feature: they obtain at most 85.10% of accuracy, combining the very deep CNN descriptors and tf-idf.

⁵Dataset can be found at <http://visiir.lip6.fr/>

In [23], the authors use a pre-trained Deep CNN *DCNN* for feature extraction. The DCNN, called “OverFeat”,⁶ was trained on ImageNet and is composed of 19 layers. The authors add more conventional image features to obtain feature vectors composed of:

1. a variant of the Histogram of Oriented Gradients *HOG* called “Root Hog” that is an element-wise square root of the L1 normalized HOG
2. mean and variance values of each channel of the RGB representation value of pixels from each of 2*2 block
3. the last two layers of the DCNN

The three descriptors are then encoded in a fisher vector. Using SVM, the authors obtain 72% of accuracy for UEC-FOOD 100.

In [24], the authors use a fine-tuned pre-trained DCNN with the large-scale ImageNet dataset for food recognition. The authors obtain 79% average accuracy for UEC FOOD 100 and 67% for UEC FOOD-256.

In [13], the authors also use a fine-tuned pre-trained Deep Neural Network and obtain 63% accuracy on UEC FOOD-256. Their neural network is fine-tuned on multiple food datasets (UEC FOOD 256, Food 101 and EgocentricFood).

2.3 Food log application and intake estimation

FoodLog⁷ is a website that enables the user to upload pictures of its daily meals to be archived and processed. The goal of this application is to assist the user to keep notes of their meals and balance the nutritional values coming from different kinds of food.

⁶Can be found <http://cilver.nyu.edu/doku.php?id=code:start>

⁷<http://www.foodlog.jp>

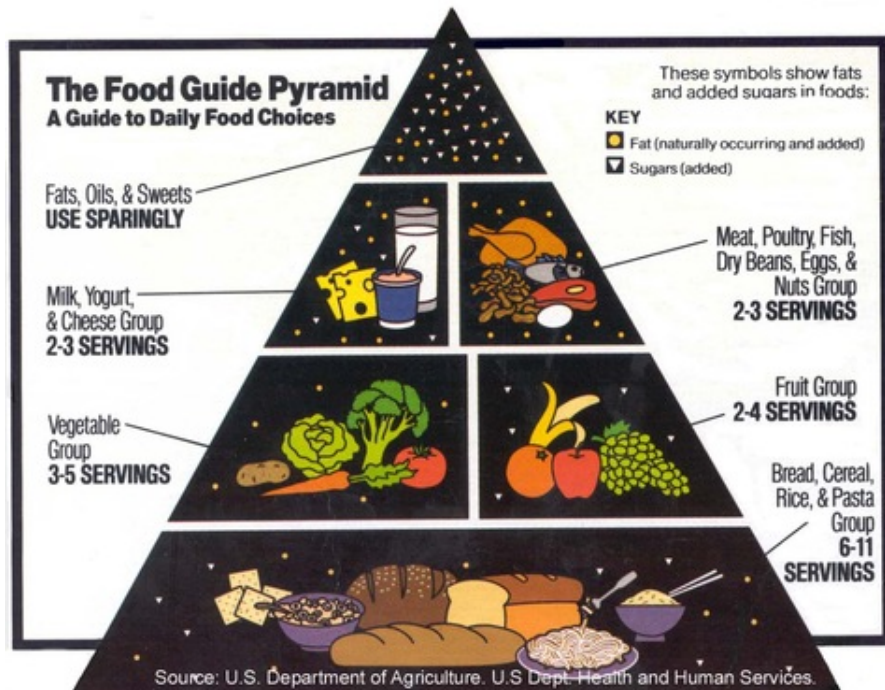


Figure 2.1: USDA MyPyramid original logo. Source Wikipedia.

In [25], the images containing food items are identified by exploiting features related to the HSV and RGB colour domains, as well as the shape of the plate. A SVM classifier is trained to detect food images. More specifically, the images are divided in 300 blocks and each block is classified as “non-food” (discarded block) or one of the nutritional categories described in the “MyPyramid” model ⁸.

MyPyramid [26] was designed by the United State Department of Agriculture *USDA* in 2005 and was replaced in 2011 by “MyPlate” ⁹ [27]. This dietary model is composed of 5 kinds of food: grains, vegetable, meals and beans, milk and fruit. For each group, a recommended intake per day is associated, Fig. 2.1. Quantity is categorized by “servings” *SV*, making it simpler to compute and keep log.

In [28] the Support Vector Machine is replaced by a Bayesian Framework *BF* to im-

⁸<http://www.mypyramid.gov>

⁹<http://www.choosemyplate.gov>

prove the classification, taking into account the previous picture of a specific user to update the classifier. The BF is based on the Gaussian Naive Bayesian (suppose independence between every pair of features and the distribution of each feature is assumed to be Gaussian). The BF takes into account the estimation using colour moments and Bag-Of-Feature of SIFT, the prior distribution and the mealtime category (breakfast, lunch and dinner). The team further improve their accuracy in [29]. Kagaya et al. use a Convolutional Neural Network [CNN] to detect and classify food from a small subset of image loaded in the FoodLog system. Compared to the other conventional methods (use of a feature descriptor such as Bag-of-Words with a classifier, e.g. SVM) described previously, the CNN showed a significantly higher accuracy.

An other method to estimate the food intake is to evaluate the food volume.

In [21], the authors presents a method that use the depth information of the picture. Once the food has been classified, the area of the food container (bowl, plate) and the depth value of the contained food is computed to obtain the food volume. Yet, this technique is still limited as it can only be used for non-transparent food, i.e it can't detect some food item such as water or cooked rice, and force the user to have a depth camera (such as Kinect).

Without depth information, the volume can also be estimated as in [30]. Almaghrabi et al. presents a novel food recognition system that is able to estimate of the nutrition intake. Moreover, they develop a mobile application to easily take pictures and keep track of the user's diet. To measure the food intake, authors compare before and after eating pictures and use the thumb as the calibration system (it supposes a one-time calibration to know the size of the thumb of the user). The process to show the intake is:

1. the user takes food pictures
2. get the contour of each picture

3. recognition of the food using colour, shape and size features with SVM.
4. volume calculation, that is computed in two steps:
 - (a) user takes a picture from above. Then, the food shape is divided into known shape (rectangle, circle, triangle ...) to compute the area.
 - (b) user takes a second picture from the side. This is used to compute the height of the food and calculate the overall volume.

The system assumes that the plate is white and round.

5. use a nutrition database to obtain the average calories

If the user has not eaten everything, the entire must be repeated. The drawbacks of this method is the user have to take several pictures, with one's thumb each time and it has been tested with a limited set of simple food types.

In [31], the authors develop a mobile application to keep food records of a user that is taking pictures of one's meal. Their method can detect multiple food items in one picture. They use a colour marker (color chequerboard) as an illumination and size indicator. As in [30], images obtained before and after foods are eaten are used to estimate the amount of food consumed.

When the user upload a picture, it is segmented, then classified by a back-end server. The estimation (labelled image with food type and volume) are sent back to the user for confirmation.

For segmentation, the authors use connected component analysis, active contours, and normalized cuts. Then, colour and texture features are extracted to feed a SVM classifier.

The authors use:

- Gabor filters. Gabor filters describe properties related to the local power spectrum of a signal and have been used for texture analysis

- 2-D colour histograms of the a^* and b^* channels of the CIELab representation.
Values are corrected using the colour marker

For the volume estimation, the authors use a 3-D volume reconstruction process. The food area is partitioned and assigned to “geometric classes”, each with their own sets of parameters.

They evaluate their segmentation and classification methods on a very small dataset composed of 63 images and 19 classes. The authors obtain an average accuracy of 89%.

In [32], their method is named “multiple hypotheses segmentation and classification” *MHSC*. It is an iterative algorithm composed of a segmentation, description (extraction of features) and classification steps.

For segmentation, the authors first detect salient region, using Canny edge and colour distribution to reject background. Then, they apply a multi-scale segmentation using normalized cut. Small segmented regions are discarded.

On the selected region, the authors used a mixed of global descriptors (first and second moment of each channel for RGB, YCbCr, $L^*a^*b^*$, and HSV colour spaces, first and second moment of the entropy in RGB, predominant colour descriptor, entropy and two first moments of the Gradient Orientation Spatial-Dependence Matrix, entropy categorization and fractal dimension estimation and estimation of the fractal dimension of the response of different Gabor filter) with local feature (multi Bag-Of-Words using SIFT for RGB, SURF for RGB, SIFT for each channel of the RGB representation and steerable filters).

Each of the 12 descriptor, global and local, is classified independently and assigned a confidence score. A late fusion function (either maximum confidence score or majority vote) is used to decide the final class. For classification, the authors use K-NN and SVM.

If the total score is inferior to a certain threshold, the overall process is repeated. The confidence score of the previous step is used to improve the segmentation.

Applied on a dataset composed of 83 labels (79 food classes plus “utensils”, “glasses”, “plates”, and “plastic cups” classes), each class having at least 30 images, they obtain a top-8 accuracy of 75%, using K-NN with the maximum confidence score.

In [12], the authors propose a food recognition system named **FoodCam** to identify food items of a picture. The presented process is used on a mobile application, the user taking a picture that is transferred to a sever, processed and results are displayed.

The first step is to detect potential region with multiple object detection algorithms. Then, for these regions, several features are extracted and used to feed SVM with Multiple Kernel Learning *MKL* method. To detect candidate regions, the authors use:

- Felzenszwalb’s deformable part model (DPM), based on Histogram of Oriented Gradients (HOG).
- a circle detector: the image is converted to a gray-scale, contour are extracted using the Canny Edge Detector and circles detected by the Hough Transform
- JSEG region segmentation: segment region based on colour. It only keeps circular regions.
- whole image, for picture with one large dish

Then, it aggregates all the candidate regions to get the bounding box of each food item.

For each region, it extracts multiple common features:

- Bag of Feature of SIFT and C-SIFT (sift with colour invariant characteristics)
- Spatial pyramid representation: object regions are divided by hierarchical grids. In this paper, the three level pyramid is used: 1×1 , 2×2 , 3×3 . For each grid, a BoF vector is extracted
- Histogram of Oriented Gradient (HOG)

- Gabor texture

After extraction of the feature vectors from each candidate region, a linear SVM trained by MKL is used (χ^2 kernel). Their methods were evaluated on UEC-FOOD 100. For multiple food item images, they obtain 55.8% classification rate and 68.9% for single food item pictures.

In [33], the authors develop a mobile real-time food recognition system for calorie and nutrition estimation. Contrary to the previous paper, all the calculation are realised on the user smartphone. The recognition takes less than 1 second thanks to the multi-core architecture of modern smartphones. The user takes a picture and draws bounding boxes around food items. Then, the system refine the segmentation based on the users' rough demarcation using Grabcut. For each item, it extracts image features and classify the image among the one hundred food classes using a linear SVM. Then, the top five food candidates are shown and the user can select one of the proposition. This recognition is updated every one second, the direction arrow as presented in Fig. 2.2 being displayed to help the user improve the result by changing the camera position and direction. To estimate the most suitable direction, the authors use the Efficient Sub-window Search method, a recent and powerful window search algorithm used in object detection. The mobile application keep records of all the pictures and their approved classification and labelled with the volume estimation. Food intake is estimated thanks to a slider on the bottom-left of the screen.

Two different descriptors are used:

- bag-of-feature, SURF for detection and description, and colour histogram with the χ^2 kernel feature map
- HOG and a colour patch descriptor (mean and variance of RGB values on a 2×2 blocks of pixel) encoded using Fisher Victor, a patch encoding strategy using

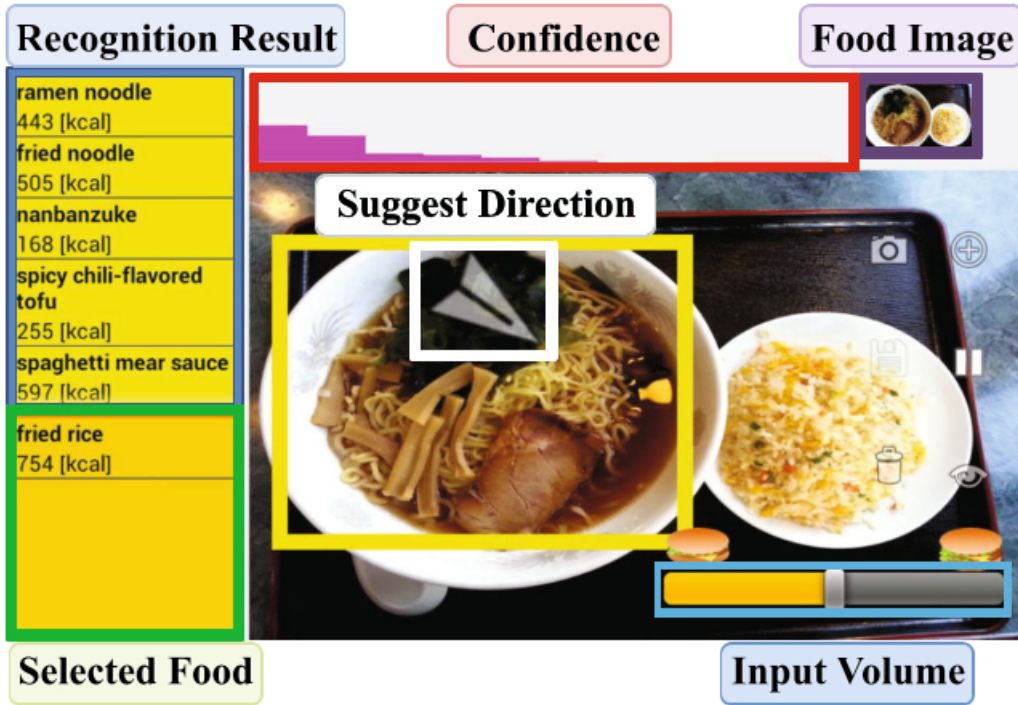


Figure 2.2: Annotated screenshot of the FoodCam application. Source [33].

Gaussian mixture models.

The authors evaluate these two methods on UEC-FOOD 100. Taking the top 5 classes, they obtain 79% classification accuracy for colour patches and 68% for the other.

In [34], the authors develop an application to recognize food items from an image taken by the user in a restaurant. It uses some contextual data (the geolocalisation) to improve the classification. Indeed, they use geolocalisation to get the menu from internet and query Google Search to get images (extract the top 50 pictures) of 15 dishes from the menu. These images are used as weakly-labelled training pictures to improve the recognition accuracy.

The first step is the segmentation to localize the food and ignore the background through hierarchical segmentation. Then, colour moment invariants, hue histograms, Bag of Words of SIFT, RGB SIFT (SIFT component for each RGB channel), C-SIFT (a color

invariant SIFT), Opponent-SIFT (SIFT on colour-opponent channels) are used as feature descriptors. For the 4 SIFT representations: they build a codebooks of 100 000 visual words (using k-means clustering, $k = 1000$) to build Bag-of-Word histogram.

Then, for the image classification, they adopt the SMO-MKL (Sequential minimal optimization - Multiple kernel learning) multi-class SVM (preceded by χ^2 kernel) methods.

It is applied on these two datasets:

- PFID to compare to existing recognition systems. Their method obtain 48.5% accuracy.
- in-house dataset consisting of images from 10 restaurants (divided in 5 different types of food: American, Indian, Italian, Mexican and Thai). It is made up of 600 pictures, 300 taken with a smartphone, 300 with Google glasses. The overall average accuracy is 63.33%, only 15.67% without localization.

Chapter 3

Feature descriptor

Image classification studies algorithms to regroup related data into a finite set of categories. It can be based on a priori knowledge (supervised learning) or on clustering algorithms to automatically separate the training data into categories (unsupervised learning).

Supervised classification typically employs two phases of processing: training and testing. In the training phase, characteristics are extracted to find rules to distinguish classes (the group of each set of data is already known). In the subsequent phase, these rules are used to classify the data.

A common representation of the data is to use a feature vector (x_1, x_2, \dots, x_n) , i.e. a list of n values corresponding to a point. Each vector is associated a label y that is predicted. Thus, the goal of the classifier is to find a mapping, a function to pass from the feature vector to the label. Usually, the function is an approximation that minimize the error.

Thus, the description is extremely important. For a computer, a picture is represented as a 2-D or 3-D array. To facilitate the classification, feature descriptor extract derived values (the features), calculated to be more informative and invariant to some common picture transformations.

As such, colour is one of the key components of a food item, thus it is widely applied

for classification. Colour statistics are commonly used, such as the first and second moment values for different channels. It can be computed for multiple colour representations (RGB, HSV, grey, YCrCb or L*a*b* space).

Another import feature of food is the texture. Numerous texture descriptors can be used such as Gabor Filters or Local Binary Pattern.

3.1 Local binary pattern

Local binary pattern is a visual descriptor for texture composition of an image, first presented in 2002 in [35] by Ojala et al. (although the concept of LBPs were introduced as early as 1993).

3.1.1 Gray-scale LBP

The Fig. 3.1 represents an example of the LBP in which the LBP code of the centre pixel (in red color and value 20) is used as a local intensity threshold : the neighbour pixels whose intensities are equal or higher than the centre pixel's are labelled as "1"; otherwise as "0". Then, starting always from the same point, we can transform this binary string to decimal and is used to describe the central pixel. In this example we start at the top-right point and work our way clockwise accumulating the binary string as we go along and obtain the value 24.

Given a pixel $c = (x_c, y_c)$, the value of the *LBP* code of c is defined as:

$$LBP_{P,R}(x_c, y_c) = \sum_{p=0}^{P-1} s(g_p - g_c)2^p$$

where:

- p is a neighbour pixel of c and the distance from p to c does not exceed R . Thus, R

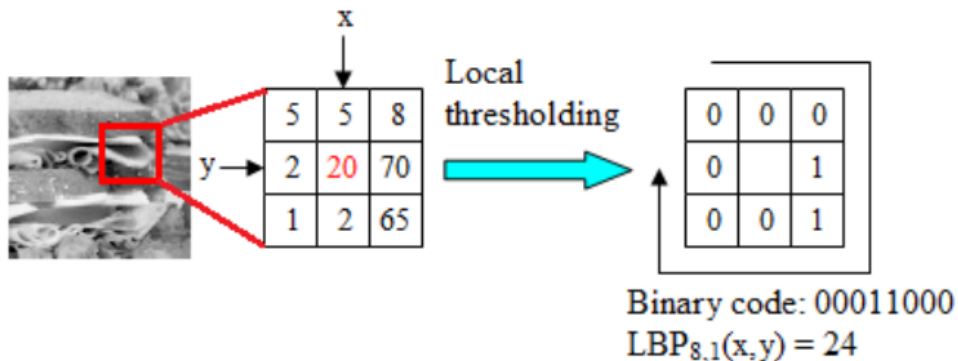


Figure 3.1: Illustration of the LBP descriptor's process. Source [35]

is the radius of a circle centred in c and P is the numbered of sampled points.

- g_p and g_c are the grey values (intensities) of p and c
- $s(x)$ is the function defined as:

$$s(x) = \begin{cases} 1 & \text{if } x \geq 0 \\ 0 & \text{otherwise} \end{cases} \quad (3.1)$$

In Fig. 3.1, R and P are 1 and 8 respectively.

The number of histograms bins for $LBP_{P,R}$ is 2^P .

3.1.2 Uniform LBP

This algorithm has been enhanced to make it rotation invariant. Still in [35], Ojala et al. introduce the notion of uniform LBP. A LBP is considered to be uniform if it has at most two bitwise transitions (0 to 1 or 1 to 0 transitions in the binary word).

For example, the pattern *01000000* (2 transitions) and *11111110* (1 transition) are both considered to be uniform. For a $LBP_{P,R}$, there is $p + 1$ possible uniforms.

Non-uniform LBP are considered as noise and are assigned the same constant value.

Thus, for uniform LBP, we use the formula:

$$LBP_{P,R}^{uni}(x_c, y_c) = \begin{cases} \sum_{p=0}^{P-1} s(g_p - g_c)2^p & \text{if uniform} \\ P + 1 & \text{otherwise} \end{cases}$$

3.2 Colour descriptor

3.2.1 Colour histogram

HSV space is composed of:

- **Hue** channel: represents the dominant spectral component—colour in its pure form, as in green, red, or yellow
- **Saturation** channel: represents the white added to the pure color (the Hue)
- **Value** channel: represents the brightness of the colour

Hue and Saturation corresponds to the chromaticity of the colour. For the joint histogram (2D histogram), the H and S channels are used as value is dependant of the condition where the picture were taken, thus is not interesting. The coordinate system is cylindrical, and is often represented by a six-sided inverted pyramid (see Fig. 3.2).

3.2.2 Colour moments

3.2.3 The first two moments

For a discrete random variable X , the first two moments are defined as:

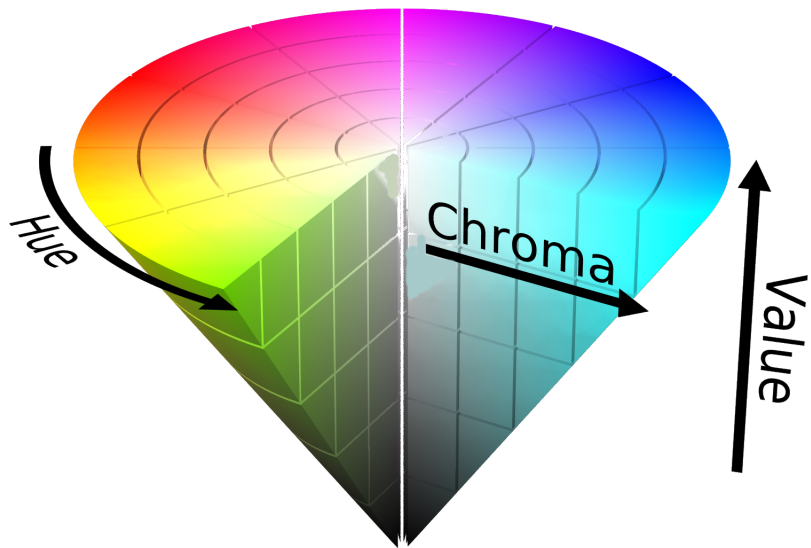


Figure 3.2: Pyramid representation of the HSV channels. Source wikipedia

- **Expected value:**

$$\mathbb{E}[X] = \mu = \sum_{i=1}^n p_i x_i$$

- **Variance:**

$$\text{Var}(X) = \mathbb{E}[(X - \mathbb{E}[X])^2] = \sum_{i=1}^n p_i(x_i - \mu)^2$$

3.2.4 Hu moments

Raw moments

For a two-dimensional continuous function $f(x,y)$ the moment (sometimes called “raw moment”) of $(p+q)$ th order is defined as:

$$M_{pq} = \int_{-\infty}^{\infty} \int_{-\infty}^{\infty} x^p y^q f(x,y) dx dy$$

for p and $q \in \mathbb{N}$.

Central moments

And the central moments are :

$$\mu_{pq} = \int_{-\infty}^{\infty} \int_{-\infty}^{\infty} (x - \bar{x})^p (y - \bar{y})^q f(x, y) dx dy$$

with $\bar{x} = \frac{M_{10}}{M_{00}}$ and $\bar{y} = \frac{M_{01}}{M_{00}}$

Normalized central moments

The normalized central moments are:

$$\eta_{ij} = \frac{\mu_{ij}}{\mu_{00}^{\gamma}}$$

where $\gamma = 1 + \frac{i+j}{2}$ for $i + j \geq 2$.

Definition of the Hu moments

On the base of those Moments, Hu in [36] introduced 7 Moments which are invariant for translation, rotation and resizing:

$$I_1 = \eta_{20} + \eta_{02}$$

$$I_2 = (\eta_{20} - \eta_{02})^2 + 4\eta_{11}^2$$

$$I_3 = (\eta_{30} - 3\eta_{12})^2 + (3\eta_{21} - \eta_{03})^2$$

$$I_4 = (\eta_{30} + \eta_{12})^2 + (\eta_{21} + \eta_{03})^2$$

$$I_5 = (\eta_{30} - 3\eta_{12})(\eta_{30} + \eta_{12})[(\eta_{30} + \eta_{12})^2 - 3(\eta_{21} + \eta_{03})^2]$$

$$+ (3\eta_{21} - \eta_{03})(\eta_{21} + \eta_{03})[3(\eta_{30} + \eta_{12})^2 - (\eta_{21} + \eta_{03})^2]$$

$$I_6 = (\eta_{20} - \eta_{02})[(\eta_{30} + \eta_{12})^2 - (\eta_{21} + \eta_{03})^2] + 4\eta_{11}(\eta_{30} + \eta_{12})(\eta_{21} + \eta_{03})$$

$$I_7 = (3\eta_{21} - \eta_{03})(\eta_{30} + \eta_{12})[(\eta_{30} + \eta_{12})^2 - 3(\eta_{21} + \eta_{03})^2]$$

$$- (\eta_{30} - 3\eta_{12})(\eta_{21} + \eta_{03})[3(\eta_{30} + \eta_{12})^2 - (\eta_{21} + \eta_{03})^2]$$

3.3 Bag-of-Words

3.3.1 Process

Bag-of-Words *BoW*, also called Bag of features, is a feature descriptor method inspired by information retrieval from textual documents.

As illustrated in Fig. 3.3, the main steps are:

- detecting keypoints on each picture. In my case, I use a dense grid of evenly spaced points at a fixed scale and orientation.

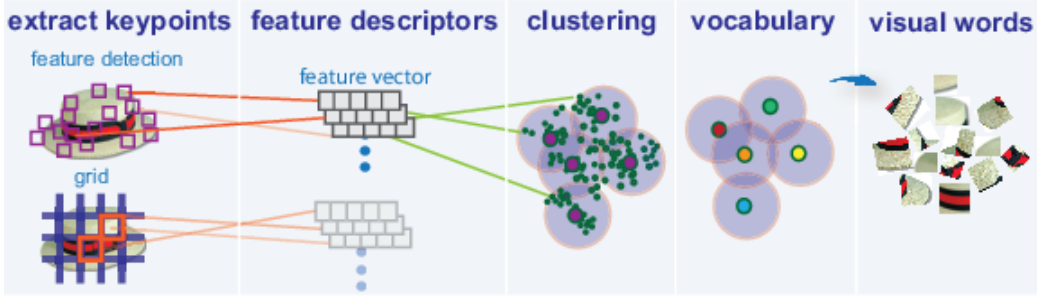


Figure 3.3: Illustration of the Bag-Of-Visual-Words model. Source MathWorks

- describing each keypoints, i.e. extract a feature vector on a neighbourhood of pixels.
SIFT, HOG and SURF are common descriptors.
- Generating a fix number of visual words that compose our codebook.
- We express each image as an histogram of these words' appearance.

The combination of a dense grid and SIFT is commonly called dense SIFT. It has been showed to have greater accuracy than using SIFT for keypoint detection and description.

3.3.2 SIFT

Scale-Invariant Feature Transform *SIFT* is an algorithm used for detection and description of local feature created by Lowe in 2004 [37].

The major stages of the algorithm are:

1. Scale-space extrema detection: The scale space of an image $L(x, y, \sigma)$ is defined as the product of the convolution of a Gaussian filter $G(x, y, \sigma)$ and an image $I(x, y)$:

$$L(x, y, \sigma) = G(x, y, \sigma) * I(x, y)$$

where $*$ is the convolution at (x, y) and $G(x, y, \sigma) = \frac{1}{2\pi\sigma^2} \exp(-(x^2 + y^2)/2\sigma^2)$.

Laplacian of Gaussian $\sigma^2 \nabla^2 G$ produced the most stable image features but are expensive to compute, thus it is approximated as an Difference of Gaussian (scale-normalized LoG for scale-invariance)

$$G(x, y, k\sigma) - G(x, y, \sigma) \approx (k - 1)\sigma^2 \nabla^2 G$$

As presented in Fig. 3.4, pyramid of DoG for each octave of scale space is computed: the initial image is repeatedly convolved with Gaussian filters for different values of σ to produce a list of scale space. Adjacent Gaussian images are subtracted to produce the Difference-of-Gaussian.

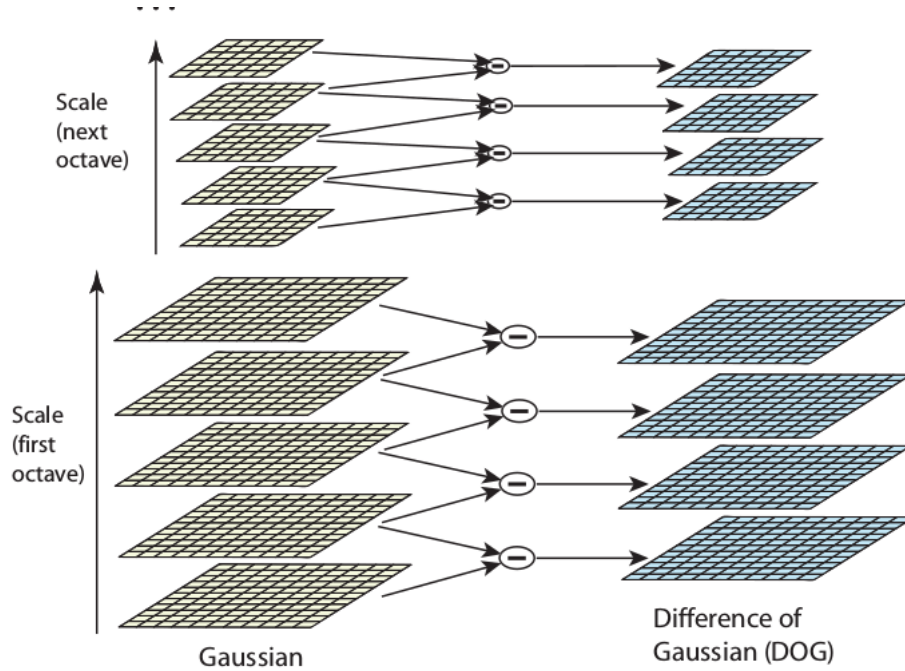


Figure 3.4: Illustration of the difference of Gaussian over multiple octave. Source [37]

2. Keypoint localisation: In order to detect the local maxima and minima of $D(x, y, \sigma)$, each sample point is compared to its eight neighbours in the current image and nine neighbours in the scale above and below. Low contrast and edge keypoints are

filtered.

3. Orientation and magnitude assignment: to obtain an orientation invariant descriptor, each keypoint is assigned a consistent value based on local image properties. Then, the keypoint descriptor can be represented relative to this orientation.

The magnitude and orientation are defined as:

$$m(x,y) = \sqrt{(L(x+1,y) - L(x-1,y))^2 + (L(x,y+1) - L(x,y-1))^2}$$

$$\theta(x,y) = \tan^{-1}\left(\frac{L(x,y+1) - L(x,y-1)}{L(x+1,y) - L(x-1,y)}\right)$$

4. Keypoint descriptor: the local image gradients of a keypoint as presented in Fig. 3.5 are computed and accumulated in a histogram. An additional Gaussian weighting function is applied to give less importance to gradients farther away from the keypoint centre.

Usually, SIFT is evaluated at 8 orientation planes over a 4×4 neighbourhood giving a 128-dimension feature vector

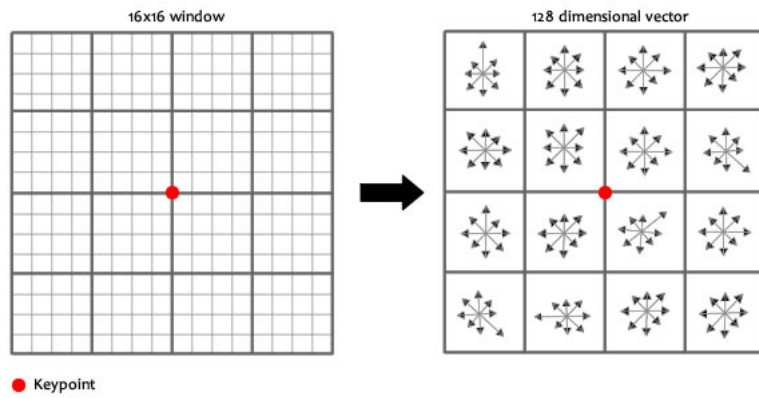


Figure 3.5: Illustration of SIFT as a local image descriptor. Source [37]

As proven by Lowe in the paper [37], this method is invariant to translation, scaling

and rotation of the picture and is robust to illumination changes, addition of noise, change in the 3-D viewpoint and local geometric distortion.

Multiple variant of SIFT exists. Colour SIFT computes the SIFT in the same manner than the grey scale, except that it does it for each channel independently. Root SIFT is a simple variant of SIFT, presented in [38]. When the SIFT descriptors as been computed for each keypoints, we apply an element wise square root of the L1 normalized SIFT vectors

However the SIFT algorithm is quite slow method. That is why in [39], Bay et al. present a faster algorithm base on the SIFT approach - **Speeded Up Robust Features SURF**.

3.3.3 K-mean clustering

Given a set of observations (x_1, x_2, \dots, x_n) , where each observation is a real vector, k -means clustering aims to partition the n observations into k ($k \leq n$) sets $S = S_1, S_2, \dots, S_k$ so as to minimize the within-cluster sum of squares (sum of distance functions of each point in the cluster to its closest centre K). In other words, its objective is to find:

$$\arg \min_S \sum_{i=1}^k \sum_{x \in S_i} \|x - \mu_i\|^2 \quad (3.2)$$

Problem, the exact solution is a NP hard problem. That's why, we can use Lloyd's heuristic algorithm to compute an estimation.

It is an iterative method that find a local minima of the Eq. 3.2:

1. A set of k initial “means” is chosen randomly within the data domain $M = \{m_1, m_2, \dots, m_k\}$

2. Then, k clusters are created by associating every observation with the nearest mean.

$$\forall i \in \{1, \dots, k\}, S_i^{(t)} = \{x_p : \|x_p - m_i^{(t)}\|^2 \leq \|x_p - m_j^{(t)}\|^2 \forall j \in \{1, \dots, k\}\}$$

3. The centroid of each of the k clusters becomes the new mean.

$$\forall i \in \{1, \dots, k\}, m_i^{(t+1)} = \frac{1}{|S_i^{(t)}|} \sum_{x_j \in S_i^{(t)}} x_j$$

4. Repeats step 2 and 3 until M not longer changes.

The centroid results and number of iterations are highly dependant of the initial centroid. As a result, the computation is often done several times, with different initialisations.

To help to overcome this issue, the “kmeans++” initialisation scheme is often used, which has been described by Arthur et al. in [40]. This method initializes the centroids to be (generally) distant from each other, leading to provably better results than random initialization.

Chapter 4

Machine learning

As classifiers, the most encountered algorithms in the literature are employed: Random Forest, Support Vector Machine and Convolutional Neural Network.

4.1 Decision tree and random forest

Decision tree is a simple learning method that can be used for classification or regression. The implementation used of decision tree is based on the CART (Classification and Regression Tree) algorithm.

A decision tree is recursively partitioning the space in a left P_{left} and right P_{right} partitions such that the samples with the same labels are grouped together, i.e. the generated sets with the smallest impurity.

It continues to split until the impurity can't be reduced or some pre-set stopping rules are met. Alternatively, the data are split as much as possible and then the tree is later pruned.

Since the set of splitting rules used to segment the predictor space can be summarized in a tree, these types of approaches are known as decision tree methods. The Figure 4.1

illustrate a toy example of decision tree.

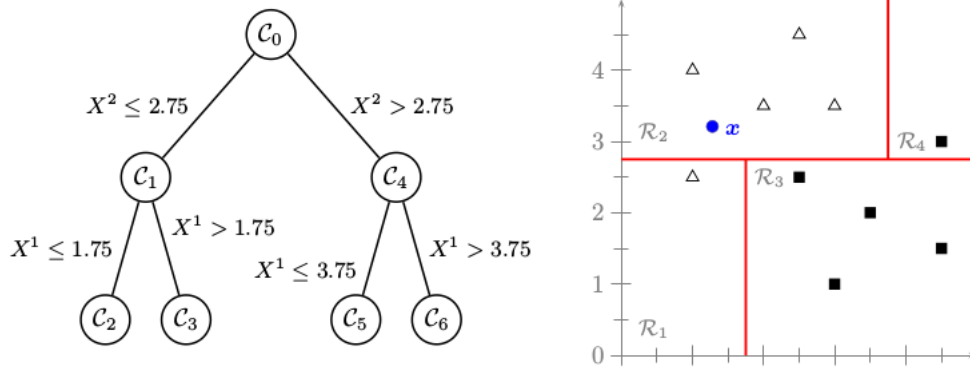


Figure 4.1: Decision tree of depth two for ten elements (X^1, X^2) belonging to the black square and white triangle classes

The most used impurity measure's functions are:

- **Gini:**

$$H(X_m) = \sum_k p_{mk}(1 - p_{mk})$$

- **Cross-entropy:**

$$H(X_m) = - \sum_k p_{mk} \log(p_{mk})$$

To avoid overfitting, keep the decision tree as simple as possible.

Random forest or Decision forest is build from a number of decision trees. The prediction of the ensemble is given as the averaged probability of the individual classifiers. Each tree is trained on a random subsets of the training data.

When building these decision trees, each time a split in a tree is considered, a random sample of m predictors is chosen as split candidates from the full set of n features. A typical value of m is $m \approx \sqrt{n}$.

4.2 Support Vector Machine

Support Vector Machine *SVM* is a widely used method for classification and regression.

4.2.1 Linear SVM

Hard margin

A support vector machine constructs a hyper-plane or a set of hyper-planes in a high or infinite dimensional space. Intuitively, a good separation is achieved by the hyper-plane that has the largest distance to the nearest training data points of any class (so-called functional margin), since in general the larger the margin the lower the generalization error of the classifier.

For a 2 classes (value represented as -1 and 1), the hyperplane must verify:

$$\vec{x}_i \cdot \vec{w} + b \geq +1 \text{ for } y_i = +1 \quad (4.1)$$

$$\vec{x}_i \cdot \vec{w} + b \leq -1 \text{ for } y_i = -1 \quad (4.2)$$

where \vec{w} is the normal to the hyperplane

Combining equation 4.1 and 4.2, we obtain:

$$\forall i \in 0, \dots, n, \quad y_i(\vec{x}_i \cdot \vec{w} + b) - 1 \geq 0$$

where $y_i = f(\vec{x}_i) = -1, 1$

Geometrically, the distance between the two hyperplanes from 4.1 and 4.2 is $\frac{2}{\|\vec{w}\|}$ (equal width to each side).

Thus, to obtain the hyperplane with the highest margin, we want to maximize:

$$\arg \max_{\vec{w}, b} \frac{2}{\|\vec{w}\|^2}$$

which is equivalent to minimize:

$$\arg \min_{\vec{w}, b} \frac{1}{2} \|\vec{w}\|^2$$

Thus, we obtain a constrained optimization problem.

Soft Margin

For the case of non-separable training sets, we introduce a penalty parameter C , $C \leq 0$ and obtain:

$$\arg \min_{\vec{w}, b, \zeta} \frac{1}{2} \|\vec{w}\|^2 + C \sum_{i=1}^n \zeta_i \text{ subject to } y_i(\vec{x}_i \cdot \vec{w} + b) \geq 1 - \zeta_i, \zeta_i \geq 0, \forall i \in [1, \dots, n]$$

The decision function for new example is:

$$f(\vec{x}) = \text{sign} \left(\sum_{s_i \in \text{support vectors}} w_i \vec{s}_i \cdot \vec{x} + b \right)$$

where the support vectors selected sub-set of the training examples that define the boundary of the hyperplane separation and hence the classification boundary.

To generalize SVM to the case of multi-class, multiple approaches are possible:

- “one-versus-one”: train a separate classifier for each different pair of labels. This leads to $\frac{N(N-1)}{2}$ classifiers
- “one-versus-all”: train a single classifier per class, with the samples of that class as

positive samples and all others as negatives

4.2.2 Non-linear SVM and kernel trick

The idea of the kernel trick is to transform the initial space to a higher dimensional space where a hyperplane can separate this data. Kernel trick: use kernel function to implicitly transform datasets to a higher-dimensional using no extra memory, and with a minimal effect on computation time: realise just a dot product.

To use the linear SVM for non-linear data: project the data in a new feature H space thanks to an application and then research for maximum margin hyperplane in H to make sure that the new problem has a unique solution, must satisfy the Mercer's condition or simply it must be a positive definite matrix

- **Linear** : $k(x, y) = \langle \vec{x}, \vec{y} \rangle + C = x^T y + C$
- **Polynomial**: $k(x, y) = (\gamma \cdot \langle \vec{x}, \vec{y} \rangle + C)^d = (\gamma \times x^T y + C)^d$
- **Radial Basis Function (RBF)**: $k(x, y) = \exp(-\gamma \|x - y\|^2)$
- **Chi-Square**: $k(x, y) = 1 - \sum_{i=1}^n \frac{(x_i - y_i)^2}{\frac{1}{2}(x_i + y_i)}$

A modified version presented in [41] of this kernel is the **Additive Chi-Square**

$$\text{kernel} : k(x, y) = \sum_{i=1}^n \frac{2(x_i - y_i)}{x_i + y_i}$$

The adjustable parameters of these kernels are d , γ , C and must be chosen according to the problem.

For food classification, the chi square kernel is the most used kernel as it is often combined with histograms. !!CITE!!

4.3 Convolutional neural network

A **Convolutional Neural Network CNN** is a variant of a Neural Network, mainly used for machine learning on pictures. It is inspired by the neural system composed of different layers (made up of multiple neurons) and communication scheme.

Each neuron receives some inputs, performs a dot product and optionally follows it with a non-linearity function. The whole network still expresses a single differentiable score function (linear or not): from the raw image pixels (the input layer) to class scores (output layer). Hidden layers separates these two layers, as described in 4.2.

A CNN (and more generally a NN) is trained by backward propagation of the errors (backpropagation), applying gradient descent that will update the weights.

It is a powerful, adaptive and noise resilient pattern recognition. The training phase is rather slow but querying it with an unseen example is fairly fast.

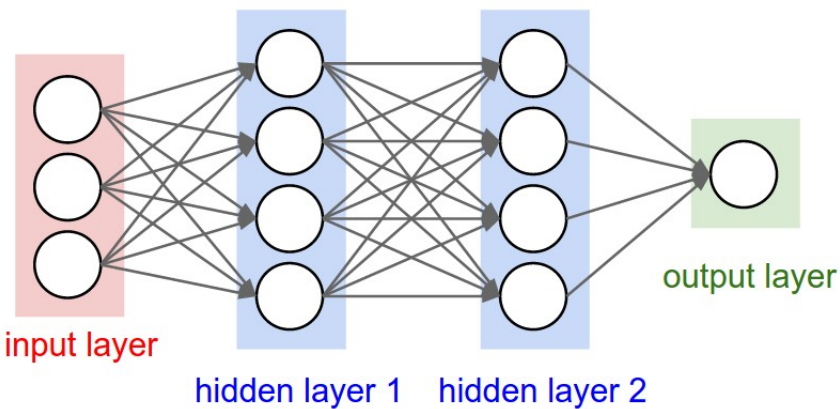


Figure 4.2: A regular 3-layer neural network. Source [42].

The Figure 4.3 is a simple CNN based on the VGG-NET structure. It is composed of the 4 most popular layers that can be found in a CNN:

- **Convolutional** : layer giving the name for this type of neural network. It convolves the input image with a set of learnable filters, each producing one feature map in

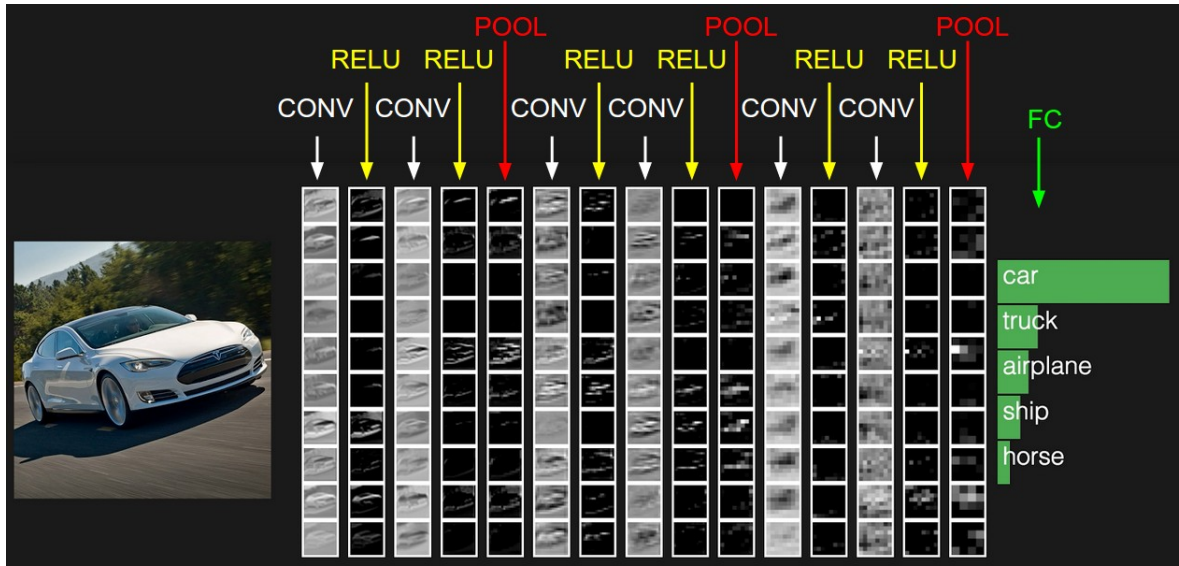


Figure 4.3: Example of a 16-layer deep convolutional neural network. The input layer is a whole picture, the output layer is the probability for each possible class. It used a succession of Convolutional, ReLU, Pooling layer with a final Fully connected one. Source [42].

the output image, i.e. it computes a dot product on a neighbourhood of pixels:

$$y_{i,j} = b + \sum_{l=0}^{n-1} \sum_{m=0}^{n-1} w_{l,m} x_{j+l,k+m}$$

with:

- $x_{i,j}$ the input activation at position (x,y)
 - $w_{l,m}$ the weights of the neuron
 - $n \times n$ is the size of the layer
 - b is the bias value
 - $y_{i,j}$ the output values of the j, k th neuron
- **Activation layer:** element wise operation.

Example of function: the **Rectified Linear Unit *ReLU*** defines as:

$$f(x) = \max(0, x)$$

- **Pooling** or subsampling layer: down sampling of the input activation size. It reduces the number of values between the input and the output values of this layer to avoid overfitting the data and reduce the computation time of the neural network.

The most common downsampling operation is the function max, giving rise to **max pooling**, here shown with a stride of 2 in Figure 4.4.

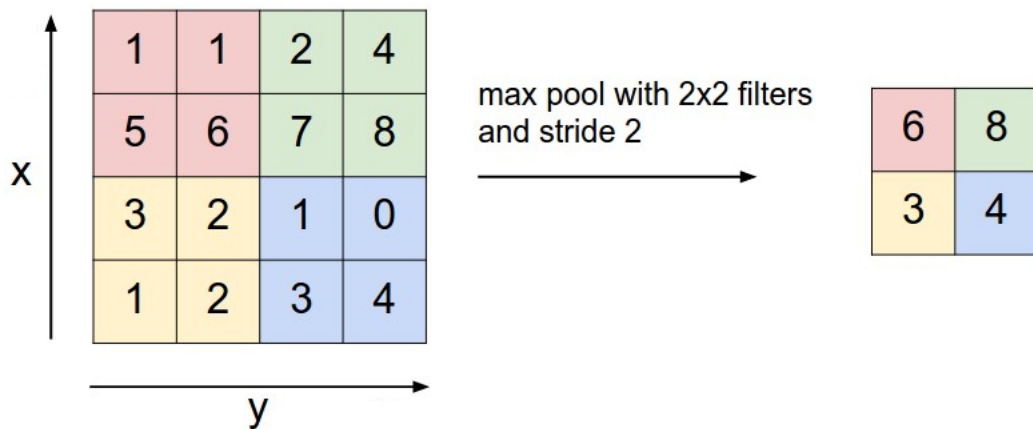


Figure 4.4: Illustration of a max pooling layer of stride 2, i.e. it selects the maximum value from a 2×2 square. Source [42].

- **Fully connected**: compute the class scores. As the name implied, this neuron is connected to all activations from the previous values. For classification, it corresponds to a loss function, a common one is the sigmoid:

$$\sigma(x) = \frac{1}{1 + \exp(-x)}$$

A CNN can also be used as a feature descriptor if we use the output of the last layers.

Chapter 5

Dataset

The image analysis approach require a dataset for training. This collection of images should include all the information (class, localisation) to enable the classification. A labelled dataset can be split to be used for the training and evaluation. Thus, the accuracy of the method can be measure.

5.1 Choice of the dataset

Numerous datasets are already existing and have been made freely available. Creating one's own dataset was an option but it would have been very time consuming and our method's result could not be compared to previous scientific papers.

To choose, a couple of criteria were defined:

- It must have a sufficient number of classes to get closer to the conditions of a food log system.
- It must have an adequate number of pictures per label to enable the classifiers to extract rules but, for technical reason, it can't exceed a few tens of thousands of images

Name	Re-lease date	Number of pictures	Type of food	Number of classes	Multiple food items
PFID [15]	2009	4545	American fast-food	101	No
UEC FOOD 100 [12]	2012	14361	Japanese	100	Yes
FIDS 30 [43]	2013	971	Fruit	30	No
ETHZ Food-101 [20]	2014	101 000	European	100	No
UPMC Food-101* [22]	2015	90 840	European	100	No
UNICT-FD889 [44]	2015	3 583	World	889	No
FooDD [45]	2015	3000	Fruit	23	Yes
UEC FOOD 256 [8]	2015	31395	World	256	Yes

Table 5.1: Summary of some available food datasets according to the criteria.

*UPMC FOOD 101 is also including the recipe for most of the pictures

- It must be composed of a general kind of food such as worldwide, Western or Asian
- It must contain pictures with multi-food items

These criteria have been defined to be reasonable cases if a food log application were to be created. As we can see in the table 5.1, UEC FOOD 256 is the dataset that best match our expectations.

5.2 UEC FOOD-100 and UEC FOOD-256

UEC FOOD-100 and **UEC FOOD-256** are datasets used for food localisation and recognition.

The UEC FOOD-100 ¹ dataset was created by Matsuda et al. from the University Electro-Communications of Tokyo in 2012 [12].

It contains 100 types of food, mainly Japanese food. Each kind is represented by at least 100 samples.

¹Dataset can be found at <http://foodcam.mobi/dataset100.html>

As presented in Fig. 5.1, a photo can contain more than one food items. The dataset contains files to indicate bounding boxes marking the location of a food items.

The UEC FOOD-256² was presented by Kawano et al. (same institute as Matsuda et al) in 2015. It contains the 100 types of food from UEC FOOD-100 plus 156 new ones. The pictures have been automatically extracted from the Internet and pre-processed.

The newly introduced food kinds are more international dishes with food from various countries such as France, Italy, the USA, China, Thailand, Vietnam, Japan and Indonesia. As for FOOD 100, every food photo has a bounding box indicating the location of the food item.

The most represented category is miso soup with 728 and rice with 620 pictures (for a list of classes, see Annexe 2).

²Dataset can be found at <http://foodcam.mobi/dataset256.html>



Figure 5.1: Pictures with multiple food items from UEC FOOD 256

Chapter 6

Methodology

As illustrated in Fig. 6.1, we have our initial dataset that we split in :

- a **validation set** (10% of the dataset) used for hyper-parameter optimization or model selection for localisation and classification
- a **train / test set** (remaining dataset) used for the localisation and classification.
The train set is used to learn the parameters of a classifier that is then evaluated on the test set (using the same dataset for learning and testing would lead to overfit the dataset and will not represent the capacity of the method to recognise new unknown element)

6.1 Hyperparameter optimization

There are numerous parameters that are part of the machine learning algorithm but are not learnt. Typical example include which kernel function used (if any) or the value of the penalty parameter C for SVM, the number of k of neighbourhoods for K-NN.

We use the exhaustive grid search method to select the parameters that have the highest

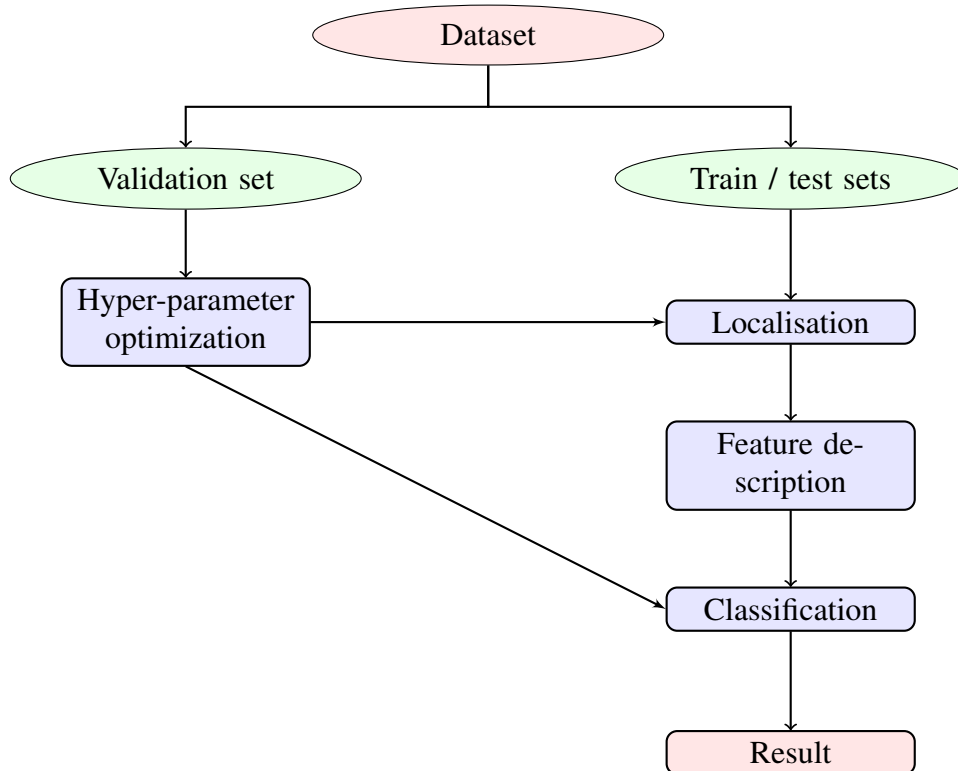


Figure 6.1: General process of the localisation and classification

performance score through 10 fold cross validation. It generates all the possible combination of parameters value and train / test the classifier.

6.2 Localisation

For localisation, a different approach from the literature has been used. The usual way is to detect area of food and non-food in a picture. Yet, it was noticed that the food items of UEC FOOD 256 and 100 tends to be in the middle and stands out. Moreover, requesting the user to take pictures that follow these characteristics is reasonable.

That's why a pre-trained CNN used for saliency detection has been used. It has been pre-trained in [46] on multiple datasets (Multi-Salient-Object, ILSVRC14). It is available

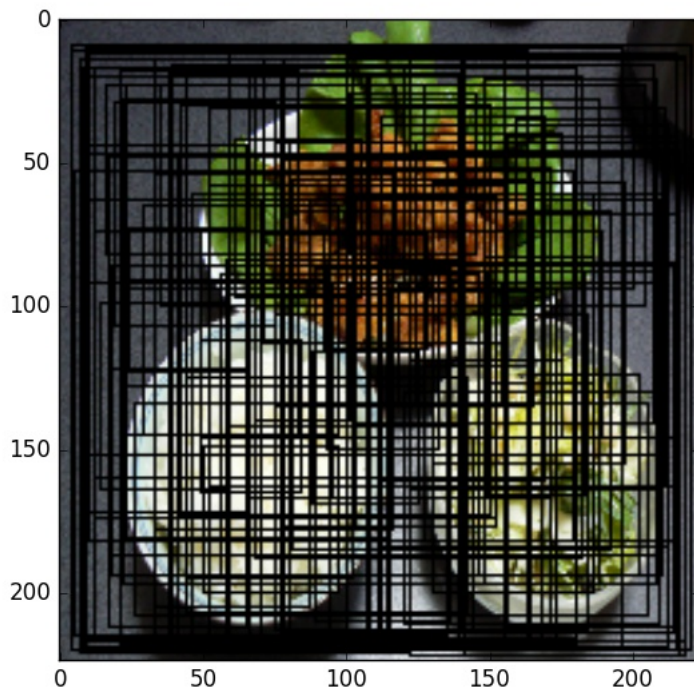


Figure 6.2: Picture of the 100 possible bounding boxes that the salient CNN will try to recognise

on this gist¹.

The CNN structure is a copy of “GoogleNet” model [14], i.e. it is composed of 22 layers, corresponding to a succession of convolutional, max pooling and activation layers, the last one being a sigmoid function.

The CNN has been pre-trained to detect the likelihood to belong to one of the 100 arbitrary bounding boxes as presented in Fig. 6.2.

Bounding boxes with a probability higher than a threshold T are selected as candidate (if no box meet this limit, the bounding box with the maximum value is selected). As can be seen in Fig. 6.3, it generates a lot of overlapping copies. That’s why, the final step of the localisation process is to discard small bounding boxes and overlapping ones (overlap

¹<https://gist.github.com/jimmie33/339fd0a938ed026692267a60b44c0c58>

higher than 30%), keeping the ones with highest probabilities.

6.3 Food recognition

6.3.1 Histograms and moments

The first feature descriptor used a combination of LBP histogram with colour moments and histogram for each picture:

1. extract a 100-bin histogram of local binary pattern on the grey scale image
2. extract a 30-by-30-bin joint colour histogram for the channel H and s of the HSV representation
3. extract the first two moments of the R, G, B, H, S and Gray channels
4. extract the 7 Hu moments

The feature vectors are then normalized to have all features centred around zero (mean equal to 0) and have unit variance (equal to 1).

Then, multiple classifiers are applied :

- decision tree
- random forest (made up of 500 trees)
- SVM

6.3.2 Bag of words

The usual process of Bag-of-Features is used:

1. detection of keypoints using a dense grid

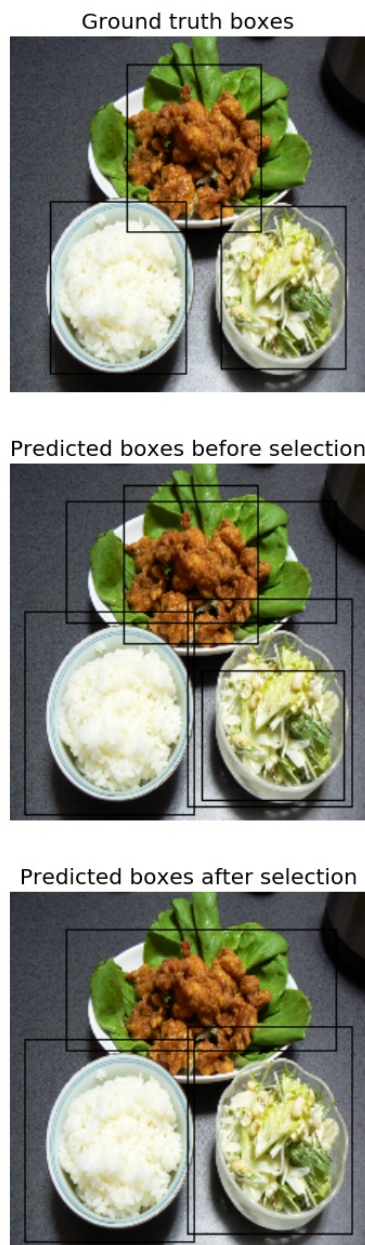


Figure 6.3: Segmentation process with: the bounding boxes (top), the candidate bounding boxes (middle), the proposed bounding boxes after overlapping suppression (bottom)

2. Root SIFT description
3. clustering using the k-means algorithm to obtain a 1000-word codebook.

Then, for each picture, we compute the histogram of occurrence counts of visual words. This descriptor is used with the SVM classifier and additive χ -squared kernel.

6.3.3 CNN as a Descriptor

As described in section 4, a CNN can be used as a feature descriptor. The pre-trained CNN was used for image recognition on ImageNet Challenge 2014 and presented in [47]. It is available on gist².

The model is an improved version of the 19-layer model used by the VGG team in the ILSVRC-2014 competition. As the CNN used for segmentation, it takes a 224×224 RGB picture as input.

The output of the layer just before the FC is used as a descriptor. Thus, each picture is described by a 4096 feature vectors.

6.4 Code

The code is freely available on Github³.

I'm using python 3.5.2 and its scientific stack based on Scipy [48]:

- Numpy [49] for N-dimensional array
- Pandas [50] for the data structure
- Scikit-image [51] and OpenCV 3 [52] for some of the image processing algorithms

²<https://gist.github.com/ksimonyan/3785162f95cd2d5fee77/>

³https://github.com/bnogaret/food_log

- Scikit-learn [53] for most of the machine learning and Caffe [54] for the convolutional neural netzork framework
- Matplotlib [55] for 2D graph generation
- Sphinx for the documentation

Chapter 7

Evaluation

7.1 Environment

All the code has been run on the “Astral” high performance computer of Cranfield’s university. The operating system is SUSE Linux Enterprise Server 11 (64 bits architecture), with a Linux 3 kernel.

The system is separated in login nodes and compute nodes. There are two “front-end” login nodes and they contain two Intel E5-2660 (Sandy Bridge - 8 cores) CPUs giving 16 CPU cores and have a total of 192 GB of shared memory. The login nodes enable the user to connect to the system and compile one’s program. There are 80 compute nodes, each node having two Intel E5-2660 (Sandy Bridge - 8 cores) CPUs. This is giving a total of 1280 available cores. Each compute node have at least accessed to 64 GB shared memory. Nodes are connected with InfinibandTM low-latency interconnect.

7.2 Segmentation metrics

To measure the precision of the localisation / segmentation algorithm, we use the metrics as defined in [56]¹.

To be considered a correct detection, the **Intersection over Union** *IoU* between the predicted bounding box B_p and ground truth bounding box B_{gt} must exceed 50% by the formula:

$$IoU = \frac{area(B_p \cap B_{gt})}{area(B_p \cup B_{gt})}$$

To simplify the calculation, this formula can be rewritten as:

$$IoU = \frac{area(B_p \cap B_{gt})}{area(B_p) + area(B_{gt}) - area(B_p \cap B_{gt})}$$

Using this metric, we can compute the precision P , the recall R and the accuracy A given by:

$$P = \frac{T_p}{T_p + F_p}$$

$$R = \frac{T_p}{T_p + F_n}$$

$$A = \frac{T_p}{T_p + F_n + F_p}$$

with:

- T_p the number of true positives (the bounding boxes correctly localised)
- F_p the number of false positives (the predicted bounding boxes incorrectly local-

¹Information on the evaluation system can be found at http://host.robots.ox.ac.uk/pascal/VOC/voc2012/devkit_doc.pdf

ized)

- F_n the number of false negative (the ground truth bounding boxes not localized)

Note that given the convention from [56], if more than one predicted bounding box overlaps the same ground truth bounding box, only one will be considered as T_P , the rest will be F_P s.

7.3 Cross validation

Cross validation is a technique used to assert the generalization to a new dataset of the different metrics used.

A common type of cross validation is the k-fold cross validation. In this method, the original sample is randomly split into k partitions of equal sized. Of these generated subsamples, a single split is used for test set, the remaining are used as training data. This last task is repeated k times, each of the k partitions being used only once for testing. The k results can then be averaged to produce a single estimation (illustrated in figure 7.1)

The advantage of this method over repeated random sub-sampling is that all observations are used for both training and testing, each observation being used for testing exactly once.

10-fold cross-validation were used for all the presented results (the most common fold value that maximises the training set size).

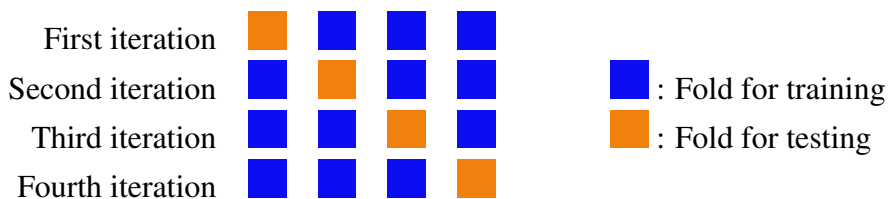


Figure 7.1: Illustration of 4-fold cross validation

7.4 Results

First, the localisation and classification processes were run independently (using the ground truth bounding box for classification).

7.4.1 Localisation

Metric (average)	My method	DCNN from [13]
Accuracy	74%	60%
Recall	74%	80%
Precision	79%	70%

Table 7.1: Average localisation accuracy result for UEC FOOD 256

The table 7.1 gathers the average accuracy, recall, precision of my localisation method using a DCNN pre-trained on salient object detection. In [13], Bolanos use a fine-tuned pre-trained Deep Neural Network and obtain around 60% of accuracy (using the same IoU over 50%). It was fine-tuned to detect bounding boxes containing food on multiple datasets.

Compare to the found literature, my method lead to a higher accuracy. It seems that the assumptions made to switch from a DCNN trained to detect food / non-food detection to salient object detection is founded. Moreover, a higher accuracy is not to the detriment of the recall or precision.

For the result of the table 7.1, we use an IoU of 50%. In Fig. 7.2, we can see that the metrics' values are greatly influenced by the threshold choose for correctness (from 73% of average accuracy with a threshold at 50% to 0% of accuracy for a threshold of 100%).

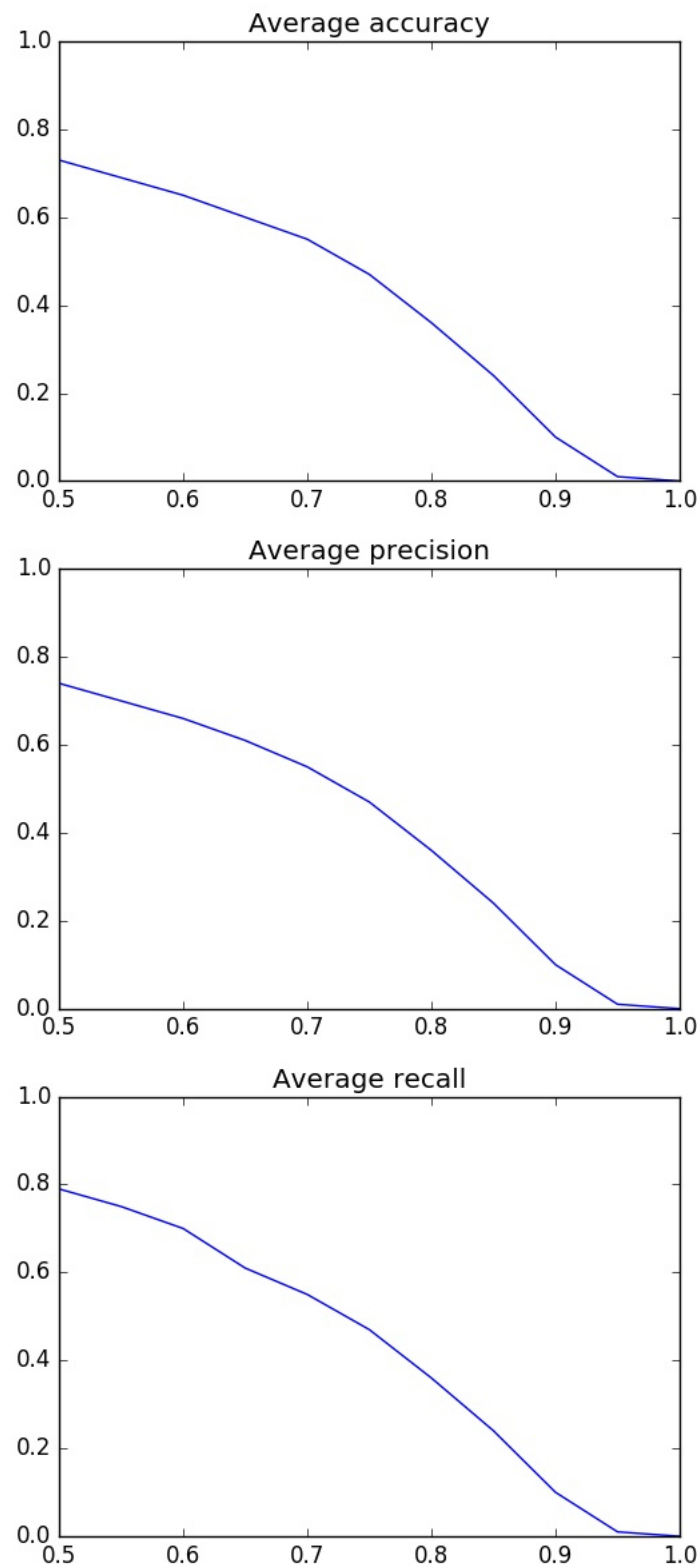


Figure 7.2: Curves of Accuracy over IoU (top), Precision over IoU (centre) and Recall over IoU (bottom)

Method	Average accuracy
CNN as descriptor + RF	40%
BoW (1000 words)+ SVM with χ^2	10%
LBP + CHM + Decision tree	5%
LBP + CHM + SVM	11%
LBP + CHM + RF	16%
DCNN from [13]	63%
DCNN from [24]	67%

Table 7.2: Average classification accuracy result for UEC FOOD 256. CHM stands for colour histograms and moments

Process	My method	DCNN from [13]
Overall	28%	37%
Localisation	74%	60%
Classification	38%	60%

Table 7.3: Average accuracy result for simultaneous localisation and recognition on UEC-FOOD 256

7.4.2 Classification

In [13], the authors use a fine-tuned pre-trained Deep Neural Network and obtain 63% accuracy on UEC FOOD-256.

In [24], the authors use a fine-tuned pre-trained Deep Neural Network and obtain 67% accuracy on UEC FOOD-256.

7.4.3 Localisation and classification

Using the segmentation and classification method with the highest accuracy, i.e. saliency detection DCNN segmenter with DCNN as a feature descriptor and random forest classifier, we present the final results fixing the IoU threshold to 50% in table 7.4. The total accuracy is 28% that is 9 points below the method presented by Bolanos et al. in 2016 [13]. The localisation process is able to find most of the items in a picture.



Figure 7.3: The five classes having the highest accuracy with (from the left to the right, starting from the highest accuracy) rice (98%), miso soup (95%), grilles pacific saury (94%), hamburger (93%), roll bread (90%)



Figure 7.4: The five classes having the lowest accuracy with (from the left to the right, starting from the lowest accuracy) tanmen (0%), Pork with lemon (0%), clear soup (1%), yellow curry (1%), grilles eggplant (1%)

As can been seen in Fig. 7.3 and 7.4, the best performing class is rice and the least one is tanmen. The possible explanations are:

- rice is the most represented food items in the dataset, maximising the size of the training sets (same for miso soup)
- rice has a specific texture and colour that is relatively invariant to the condition
- tanmen is a soup containing noodle and various vegetables. Thus, it can occur in different colour, shape and size.
- there are numerous soups in the dataset and tanmen is often confused with them.

Fig. 7.5 show the most class couples that are the most confused and it shows that clear and miso soup are often mixed up by the method.

The method were also run the segmentation and classification on UEC FOOD 100. The results are presented in table 7.4. As UEC-FOOD 256, it can be seen that the local-



Figure 7.5: The four most confused classes (with from the left to the right, starting from the lowest accuracy) clear soup and miso soup (83%), chicken rice and fried rice (54%)

Process	My method	DCNN from [11]	DCNN from [23]
Overall	33%	-	-
Localisation	67%	60%	-
Classification	50%	-	72%

Table 7.4: Average accuracy result for UEC FOOD 100

isation is better than the previous work with 67% accuracy (the result is slightly lower than UEC-FOOD 256 as the dataset has a higher proportion of multiple food items per picture). The overall accuracy is 33%.

Chapter 8

Future work

In this thesis, the problem of food image analysis has been taken into account.

After a review of the literature a localisation and classification method was proposed to detect multiple food items of a picture. The localisation process use a novel approach with a pre-trained convolutional neural network to detect salient objects and it currently outperforms the previous works on the UEC FOOD 256 and 100 datasets with respectively 74% and 60% for localisation only and 28% and 33% for the whole process.

One of the possible future area of work is using a more accurate feature descriptor and / or classifier. Compared to the literature, my food recognition accuracy is rather low. Exploring the use of new descriptors or the combination of local and global methods would be really likely to improve the recognition process. Especially, using a fine-tuned pre-trained deep convolutional neural network for food recognition seems really promising.

A different level of classification could be another area of studies. Then, the food intake estimation part could be added. It would include a calorie and nutrient evaluation or a simplified version based on “MyPyramid” or “MyPlate”. This could then easily an application to take pictures and visualize user’s record. Yet, using these intake representations

is far from allowing the system to totally replace the human.

Appendix A

Appendix

A.1 File structure of UEC-FOOD 256

The zip directory including all the files of the dataset contains, Fig. A.1:

1	114	13	145	160	176	191	206	221	237	252	37	52	68	83	99
10	115	130	146	161	177	192	207	222	238	253	38	53	69	84	category.txt
100	116	131	147	162	178	193	208	223	239	254	39	54	7	85	multiple_food.txt
101	117	132	148	163	179	194	209	224	24	255	4	55	70	86	README.txt
102	118	133	149	164	18	195	21	225	240	256	40	56	71	87	
103	119	134	15	165	180	196	210	226	241	26	41	57	72	88	
104	12	135	150	166	181	197	211	227	242	27	42	58	73	89	
105	120	136	151	167	182	198	212	228	243	28	43	59	74	9	
106	121	137	152	168	183	199	213	229	244	29	44	6	75	90	
107	122	138	153	169	184	2	214	23	245	3	45	60	76	91	
108	123	139	154	17	185	20	215	230	246	30	46	61	77	92	
109	124	14	155	178	186	200	216	231	247	31	47	62	78	93	
11	125	140	156	171	187	201	217	232	248	32	48	63	79	94	
110	126	141	157	172	188	202	218	233	249	33	49	64	8	95	
111	127	142	158	173	189	203	219	234	25	34	5	65	80	96	
112	128	143	159	174	19	204	22	235	250	35	50	66	81	97	
113	129	144	16	175	190	205	220	236	251	36	51	67	82	98	

Figure A.1: UEC-FOOD 256 list of files and directory in the root. Directories are in blue, files in white.

- “README”: file briefly describing the structure and including the license
- “category.txt”, Fig. A.2: a file associating an id (a number in $[1 - 256]$) to a class, i.e. a specific food category such as rice or pizza

id	name
1	rice
2	eels on rice
3	pilaf
4	chicken and egg on rice
5	pork cutlet on rice
6	beef curry
7	sushi
8	chicken rice
9	fried rice
10	tempura bowl
11	bibimbap
12	toast
13	croissant
14	roll bread
15	raisin bread
16	chip butty
17	hamburger
18	pizza
19	sandwiches
20	udon noodle

Figure A.2: UEC-FOOD 256 file: *category.txt*

- “**multiple_food.txt**”, Fig. A.3: a file giving the list of images containing multiple food categories

img	category1	category2	..	categoryn
1	1	42		
9	1	24		
14	1	36		
19	1	69	70	
22	1	36	67	70
25	1	36	87	
27	1	21		
28	1	36	63	87
30	1	36		
31	1	36	67	
33	1	36	60	69
37	1	56	87	
38	1	36	68	69
58	1	36		
59	1	69		
61	1	36		
62	1	36		
72	1	36	56	
81	1	89		

Figure A.3: UEC-FOOD 256 file: *multiple_food.txt*. The first column is the image file-name, the following list corresponds to each class id represented on this picture.

- 256 directories, numbered from 1 to 256. Each of this directory represents a category. It includes all the pictures associated to this class. Thus, the same image can be in multiple “class category”.

Moreover, each directory include a “**bb_info.txt**”, Fig. A.4 corresponding to the

bounding box for each picture.

A bounding box is represented by its coordinate as a (x_0, y_0, x_1, y_1) :

- (x_0, y_0) : coordinate of one of the point
- (x_1, y_1) : coordinate of the opposite point

```
img x1 y1 x2 y2
1 0 143 370 486
2 20 208 582 559
3 2 110 243 410
4 0 237 286 536
5 8 28 761 585
6 0 38 369 310
7 0 162 383 450
8 80 31 776 454
9 2 226 270 470
10 71 16 478 328
12 94 150 669 567
13 0 109 344 480
14 0 337 240 600
17 0 33 414 486
18 267 158 470 357
19 352 135 500 326
20 0 154 457 542
```

Figure A.4: UEC-FOOD 256 file: *bb_info.txt*. The first column is the image filename, the next four columns are the bounding box coordinates.

A.2 List of food categories (UEC-FOOD 256)

UEC-FOOD 100 corresponds to the first 100 categories.

Food name	Id	Number of pictures
rice	1	620
eels on rice	2	130
pilaf	3	115
chicken and egg on rice	4	121
pork cutlet on rice	5	150
beef curry	6	246
sushi	7	153
chicken rice	8	100
fried rice	9	169
tempura bowl	10	136
bibimbap	11	112
toast	12	218
croissant	13	120
roll bread	14	107
raisin bread	15	101
chip butty	16	148
hamburger	17	233
pizza	18	134
sandwiches	19	163
udon noodle	20	152
tempura udon	21	106

Food name	Id	Number of pictures
soba noodle	22	163
ramen noodle	23	353
beef noodle	24	139
tensin noodle	25	112
fried noodle	26	131
spaghetti	27	151
Japanese-style pancake	28	137
takoyaki	29	134
gratin	30	115
sauted vegetables	31	120
croquette	32	126
grilled eggplant	33	102
sauted spinach	34	102
vegetable tempura	35	115
miso soup	36	728
potage	37	113
sausage	38	118
oden	39	112
omelet	40	107
ganmodoki	41	113
jiaozi	42	167
stew	43	106
teriyaki grilled fish	44	105

Food name	Id	Number of pictures
fried fish	45	121
grilled salmon	46	116
salmon meuniere	47	104
sashimi	48	124
grilled pacific saury	49	181
sukiyaki	50	122
sweet and sour pork	51	105
lightly roasted fish	52	102
steamed egg hotchpotch	53	108
tempura	54	118
fried chicken	55	154
sirloin cutlet	56	140
nanbanzuke	57	102
boiled fish	58	109
seasoned beef with potatoes	59	116
hamburg steak	60	135
steak	61	108
dried fish	62	110
ginger pork saute	63	117
spicy chili-flavored tofu	64	120
yakitori	65	111
cabbage roll	66	107
omelet	67	131

Food name	Id	Number of pictures
egg sunny-side up	68	224
natto	69	147
cold tofu	70	158
egg roll	71	109
chilled noodle	72	117
stir-fried beef and peppers	73	107
simmered pork	74	109
boiled chicken and vegetables	75	105
sashimi bowl	76	147
sushi bowl	77	111
fish-shaped pancake with bean jam	78	122
shrimp with chill source	79	118
roast chicken	80	110
steamed meat dumpling	81	115
omelet with fried rice	82	126
cutlet curry	83	142
spaghetti meat sauce	84	125
fried shrimp	85	115
potato salad	86	128
green salad	87	342
macaroni salad	88	109
Japanese tofu and vegetable chowder	89	115
pork miso soup	90	117

Food name	Id	Number of pictures
chinese soup	91	165
beef bowl	92	167
kinpira-style sauteed burdock	93	111
rice ball	94	108
pizza toast	95	105
dipping noodles	96	126
hot dog	97	102
french fries	98	153
mixed rice	99	138
goya chanpuru	100	104
green curry	101	100
okinawa soba	102	108
mango pudding	103	103
almond jelly	104	104
jjigae	105	107
dak galbi	106	105
dry curry	107	101
kamameshi	108	101
rice vermicelli	109	101
paella	110	105
tanmen	111	111
kushikatsu	112	102
yellow curry	113	104

Food name	Id	Number of pictures
pancake	114	105
champon	115	106
crape	116	101
tiramisu	117	102
waffle	118	102
rare cheese cake	119	112
shortcake	120	103
chop suey	121	100
twice cooked pork	122	113
mushroom risotto	123	114
namul	124	108
zoni	125	117
french toast	126	102
fine white noodles	127	118
minestrone	128	104
pot au feu	129	114
chicken nugget	130	103
namero	131	111
french bread	132	105
rice gruel	133	116
broiled eel bowl	134	115
clear soup	135	115
yudofu	136	118

Food name	Id	Number of pictures
mozuku	137	101
inarizushi	138	111
pork loin cutlet	139	115
pork fillet cutlet	140	115
chicken cutlet	141	113
ham cutlet	142	114
minced meat cutlet	143	107
thinly sliced raw horsemeat	144	110
bagel	145	105
scone	146	103
tortilla	147	102
tacos	148	106
nachos	149	104
meatloaf	150	113
scrambled egg	151	101
rice gratin	152	109
lasagna	153	111
Caesar salad	154	104
oatmeal	155	117
fried pork dumplings served in soup	156	116
oshiruko or red bean soup	157	108
muffin	158	112
popcorn	159	116

Food name	Id	Number of pictures
cream puff	160	108
doughnut	161	112
apple pie	162	101
parfait	163	100
fried pork in scoop	164	113
lamb kebabs	165	115
stir-fried potato and eggplant and green pepper	166	119
roast duck	167	116
hot pot	168	107
pork belly	169	107
xiao long bao	170	114
moon cake	171	104
custard tart	172	101
beef noodle soup	173	118
pork cutlet	174	103
minced pork rice	175	111
fish ball soup	176	119
oyster omelette	177	102
glutinous oil rice	178	114
turnip pudding	179	105
stinky tofu	180	103
lemon fig jelly	181	109
khao soi	182	118

Food name	Id	Number of pictures
Sour prawn soup	183	108
Thai papaya salad	184	119
sliced Hainan-style chicken with marinated rice	185	112
hot and sour with fish and vegetable ragout	186	111
stir-fried mixed vegetables	187	112
beef in oyster sauce	188	107
pork satay	189	113
spicy chicken salad	190	103
noodles with fish curry	191	100
Pork Sticky Noodles	192	120
Pork with lemon	193	100
stewed pork leg	194	106
charcoal-boiled pork neck	195	115
fried mussel pancakes	196	103
Deep Fried Chicken Wing	197	113
Barbecued red pork in sauce with rice	198	112
Rice with roast duck	199	107
Rice crispy pork	200	117
Wonton soup	201	118
Chicken Rice Curry With Coconut	202	104
Crispy Noodles	203	100
Egg Noodle In Chicken Yellow Curry	204	110
coconut milk soup	205	111

Food name	Id	Number of pictures
pho	206	117
Hue beef rice vermicelli soup	207	114
Vermicelli noodles with snails	208	101
Fried spring rolls	209	104
Steamed rice roll	210	105
Shrimp patties	211	104
ball shaped bun with pork	212	114
Coconut milk-flavored crepes with shrimp and beef	213	111
Small steamed savory rice pancake	214	106
Glutinous Rice Balls	215	106
loco moco	216	112
haupia	217	103
malasada	218	114
laulau	219	106
spam musubi	220	111
oxtail soup	221	119
adobo	222	114
lumpia	223	110
brownie	224	108
churro	225	115
jambalaya	226	109
nasi goreng	227	110
ayam goreng	228	103

Food name	Id	Number of pictures
ayam bakar	229	114
bubur ayam	230	108
gulai	231	102
laksa	232	103
mie ayam	233	107
mie goreng	234	104
nasi campur	235	117
nasi padang	236	109
nasi uduk	237	106
babi guling or pig roast	238	108
kaya toast	239	114
bak kut teh	240	107
curry puff	241	113
chow mein	242	116
zha jiang mian	243	110
kung pao chicken	244	111
crullers	245	111
eggplant with garlic sauce	246	113
three cup chicken	247	117
bean curd or tofu family style	248	105
salt and pepper fried shrimp with shell	249	119
baked salmon	250	109
braised pork meat ball with napa cabbage	251	118

Food name	Id	Number of pictures
winter melon soup	252	118
steamed spareribs	253	116
chinese pumpkin pie	254	102
eight treasure rice	255	115
hot and sour soup	256	117

Table A.1: List of all the food categories of UEC-FOOD 256

with the number of pictures associated

Bibliography

- [1] Ali H Mokdad et al. “Prevalence of obesity, diabetes, and obesity-related health risk factors.” In: *JAMA : the journal of the American Medical Association* 289.1 (2003), pp. 76–9. ISSN: 0098-7484. DOI: 10.1001/jama.289.1.76..
- [2] Ping Zhang et al. “Global healthcare expenditure on diabetes for 2010 and 2030”. In: *Diabetes Research and Clinical Practice* 87.3 (2010), pp. 293–301. ISSN: 01688227. DOI: 10 . 1016 / j . diabres . 2010 . 01 . 026. URL: <http://dx.doi.org/10.1016/j.diabres.2010.01.026>.
- [3] Lora E. Burke, Jing Wang, and Mary Ann Sevick. “Self-Monitoring in Weight Loss: A Systematic Review of the Literature”. In: *Journal of the American Dietetic Association* 111.1 (2011), pp. 92–102. ISSN: 00028223. DOI: 10 . 1016 / j . jada . 2010 . 10 . 008. URL: <http://dx.doi.org/10.1016/j.jada.2010.10.008>.
- [4] S W Lichtman et al. “Discrepancy between self-reported and actual caloric intake and exercise in obese subjects.” In: *The New England Journal of Medicine* 327.27 (1992), pp. 1893–1898. ISSN: 0028-4793. DOI: 10.1056/NEJM199212313272701. arXiv: [arXiv:1011.1669v3](https://arxiv.org/abs/1011.1669v3).
- [5] Olga Russakovsky et al. “ImageNet Large Scale Visual Recognition Challenge”. In: *International Journal of Computer Vision* 115.3 (2015), pp. 211–252. ISSN: 15731405. DOI: 10.1007/s11263-015-0816-y. arXiv: [1409.0575](https://arxiv.org/abs/1409.0575).

- [6] Richard Hillestad et al. “Can electronic medical record systems transform health care? Potential health benefits, savings, and costs.” In: *Health affairs (Project Hope)* 24.5 (2005), pp. 1103–17. ISSN: 0278-2715. DOI: 10.1377/hlthaff.24.5.1103. URL: <http://www.ncbi.nlm.nih.gov/pubmed/16162551>.
- [7] Nir Menachemi and Taleah H. Collum. “Benefits and drawbacks of electronic health record systems”. In: *Risk Management and Healthcare Policy* 4 (2011), pp. 47–55. ISSN: 11791594. DOI: 10.2147/RMHP.S12985. arXiv: 0710.4428v1.
- [8] Yoshiyuki Kawano and Keiji Yanai. “Automatic expansion of a food image dataset leveraging existing categories with domain adaptation”. In: *Lecture Notes in Computer Science* 8927 (2015), pp. 3–17. ISSN: 16113349. DOI: 10.1007/978-3-319-16199-0_1.
- [9] R. Thendral, A. Suhasini, and N. Senthil. “A comparative analysis of edge and color based segmentation for orange fruit recognition”. In: *International Conference on Communication and Signal Processing, ICCSP 2014 - Proceedings* (2014), pp. 463–466. DOI: 10.1109/ICCSP.2014.6949884. URL: http://ieeexplore.ieee.org/xpls/abs%7B%5C_%7Dall.jsp?arnumber=6949884.
- [10] Minami Wazumi et al. “Auto-Recognition of Food Images Using SPIN Feature for Food-Log System”. In: *Computer Sciences and Convergence Information Technology (ICCIT), 2011 6th International Conference on* (2011), pp. 874–877. URL: http://ieeexplore.ieee.org/xpls/abs%7B%5C_%7Dall.jsp?arnumber=6316741.
- [11] Wataru Shimoda and Keiji Yanai. “CNN-based food image segmentation without pixel-wise annotation”. In: *New Trends in Image Analysis and Processing – ICIAP 2015 Workshops*. Vol. 9281. 2015, pp. 449–457. ISBN: 9783319232218. DOI: 10.

- 1007/978-3-319-23222-5_55. URL: http://link.springer.com/chapter/10.1007/978-3-319-23222-5%7B%5C_%7D55.
- [12] Yuji Matsuda, Hajime Hoashi, and Keiji Yanai. “Recognition of multiple-food images by detecting candidate regions”. In: *Proceedings - IEEE International Conference on Multimedia and Expo*. IEEE, July 2012, pp. 25–30. ISBN: 978-1-4673-1659-0. DOI: 10.1109/ICME.2012.157. URL: <http://ieeexplore.ieee.org/lpdocs/epic03/wrapper.htm?arnumber=6298369>.
- [13] Marc Bolaños and Petia Radeva. “Simultaneous Food Localization and Recognition”. In: (2016), pp. 2–7. arXiv: 1604.07953. URL: <http://arxiv.org/abs/1604.07953>.
- [14] C Szegedy et al. “Going deeper with convolutions”. In: *Proceedings of the IEEE Conference on Computer Vision and Pattern Recognition* (2015), pp. 1–9. DOI: 10.1109/CVPR.2015.7298594. URL: /citations?view%7B%5C_%7Dop=view%7B%5C_%7Dcitation%7B%5C&%7Dcontinue=/scholar?hl=ja%7B%5C&%7Das%7B%5C_%7Dsdt=0,5%7B%5C&%7Dscilib=1%7B%5C&%7Dcitilm=1%7B%5C&%7Dcitation%7B%5C_%7Dfor%7B%5C_%7Dview=KtmM-dAAAAAJ:JV2RwH3%7B%5C_%7DST0C%7B%5C&%7Dhl=ja%7B%5C&%7Doi=p.
- [15] Mei Chen et al. “PFID: Pittsburgh Fast-food Image Dataset”. In: *Proceedings - International Conference on Image Processing, ICIP* (2009), pp. 289–292. ISSN: 15224880. DOI: 10.1109/ICIP.2009.5413511.
- [16] Zhimin Zong et al. “On the combination of local texture and global structure for food classification”. In: *Proceedings - 2010 IEEE International Symposium on Multimedia, ISM 2010*. IEEE, Dec. 2010, pp. 204–211. ISBN: 9780769542171. DOI: 10.1109/ISM.2010.37. URL: <http://ieeexplore.ieee.org/lpdocs/epic03/wrapper.htm?arnumber=5693842>.

- [17] Wu Wen and Yang Jie. “Fast food recognition from videos of eating for calorie estimation”. In: *Proceedings - 2009 IEEE International Conference on Multimedia and Expo, ICME 2009* (2009), pp. 1210–1213. ISSN: 1945-7871. DOI: 10.1109/ICME.2009.5202718. URL: http://ieeexplore.ieee.org/xpls/abs%7B%5C_%7Dall.jsp?arnumber=5202718.
- [18] Marc Bosch et al. “Combining global and local features for food identification in dietary assessment”. In: *Proceedings - International Conference on Image Processing, ICIP*. IEEE, Sept. 2011, pp. 1789–1792. ISBN: 9781457713033. DOI: 10.1109/ICIP.2011.6115809. arXiv: NIHMS150003. URL: <http://ieeexplore.ieee.org/lpdocs/epic03/wrapper.htm?arnumber=6115809>.
- [19] Shulin Yang et al. “Food recognition using statistics of pairwise local features”. In: *Proceedings of the IEEE Computer Society Conference on Computer Vision and Pattern Recognition*. IEEE, June 2010, pp. 2249–2256. ISBN: 9781424469840. DOI: 10.1109/CVPR.2010.5539907. URL: <http://ieeexplore.ieee.org/lpdocs/epic03/wrapper.htm?arnumber=5539907>.
- [20] Lukas Bossard, Matthieu Guillaumin, and Luc Van Gool. “Food-101 - Mining discriminative components with random forests”. In: *Lecture Notes in Computer Science*. Vol. 8694 LNCS. PART 6. 2014, pp. 446–461. ISBN: 9783319105987. DOI: 10.1007/978-3-319-10599-4_29. arXiv: 978-3-319-10599-4{_\}29 [10.1007]. URL: http://link.springer.com/chapter/10.1007/978-3-319-10599-4%7B%5C_%7D29.
- [21] Mei-Yun Chen et al. “Automatic Chinese food identification and quantity estimation”. In: *SIGGRAPH Asia* (2012), pp. 1–4. DOI: 10.1145/2407746.2407775. URL: <http://dl.acm.org/citation.cfm?doid=2407746.2407775>.

- [22] Xin Wang et al. “Recipe recognition with large multimodal food dataset”. In: *2015 IEEE International Conference on Multimedia and Expo Workshops, ICMEW 2015*. IEEE, June 2015, pp. 1–6. ISBN: 9781479970797. DOI: 10.1109/ICMEW.2015.7169757. URL: <http://ieeexplore.ieee.org/lpdocs/epic03/wrapper.htm?arnumber=7169757>.
- [23] Yoshiyuki Kawano and Keiji Yanai. “Food Image Recognition with Deep Convolutional Features”. In: *ACM International Joint Conference on Pervasive and Ubiquitous Computing (UbiComp)* (2014), pp. 589–593. DOI: 10.1145/2638728.2641339. URL: <http://dx.doi.org/10.1145/2638728.2641339>.
- [24] K Yanai and Y Kawano. “Food image recognition using deep convolutional network with pre-training and fine-tuning”. In: *Multimedia Expo Workshops (ICMEW), 2015 IEEE International Conference on*. IEEE, June 2015, pp. 1–6. ISBN: 978-1-4799-7079-7. DOI: 10.1109/ICMEW.2015.7169816. URL: <http://ieeexplore.ieee.org/lpdocs/epic03/wrapper.htm?arnumber=7169816>.
- [25] Keigo Kitamura, Toshihiko Yamasaki, and Kiyoharu Aizawa. “Food log by analyzing food images”. In: *ACM international conference on Multimedia* (2008), p. 999. DOI: 10.1145/1459359.1459548. URL: <http://portal.acm.org/citation.cfm?doid=1459359.1459548>.
- [26] United States Department of Agriculture. *mypyramid.gov, steps to a healthier you.* 2005. URL: <http://www.mypyramid.gov/>.
- [27] United States Department of Agriculture. *MyPlate*. 2005. URL: <http://www.choosemyplate.gov/> (visited on 03/05/2016).
- [28] Kiyoharu Aizawa et al. “Food balance estimation by using personal dietary tendencies in a multimedia food log”. In: *IEEE Transactions on Multimedia* 15.8 (Dec. 2013), pp. 2176–2185. ISSN: 15209210. DOI: 10.1109/TMM.2013.2271474. URL:

- <http://ieeexplore.ieee.org/lpdocs/epic03/wrapper.htm?arnumber=6548059>.
- [29] Hokuto Kagaya, Kiyoharu Aizawa, and Makoto Ogawa. “Food Detection and Recognition Using Convolutional Neural Network”. In: *ACM Multimedia*. 2. 2014, pp. 1085–1088. ISBN: 9781450330633. DOI: 10.1145/2647868.2654970. URL: <http://dl.acm.org/citation.cfm?doid=2647868.2654970>.
- [30] Rana Almaghrabi et al. “A novel method for measuring nutrition intake based on food image”. In: *2012 IEEE I2MTC* (2012), pp. 366–370. ISSN: 1091-5281. DOI: 10.1109/I2MTC.2012.6229581. URL: http://ieeexplore.ieee.org/xpls/abs%7B%5C_%7Dall.jsp?arnumber=6229581.
- [31] F Zhu et al. “The Use of Mobile Devices in Aiding Dietary Assessment and Evaluation”. In: *IEEE Journal of Selected Topics in Signal Processing* 4.4 (2010), pp. 756–766. ISSN: 1932-4553. DOI: 10.1109/JSTSP.2010.2051471.
- [32] Fengqing Zhu et al. “Multiple hypotheses image segmentation and classification with application to dietary assessment”. In: *IEEE Journal of Biomedical and Health Informatics* 19.1 (Jan. 2015), pp. 377–388. ISSN: 21682194. DOI: 10.1109/JBHI.2014.2304925. URL: <http://ieeexplore.ieee.org/lpdocs/epic03/wrapper.htm?arnumber=6733271>.
- [33] Yoshiyuki Kawano and Keiji Yanai. “FoodCam: A real-time food recognition system on a smartphone”. In: *Multimedia Tools and Applications* (2014), pp. 5263–5287. ISSN: 13807501. DOI: 10.1007/s11042-014-2000-8.
- [34] Vinay Bettadapura et al. “Leveraging context to support automated food recognition in restaurants”. In: *Proceedings - 2015 IEEE Winter Conference on Applications of Computer Vision, WACV 2015*. 2015, pp. 580–587. ISBN: 9781479966820.

- DOI: 10 . 1109 / WACV . 2015 . 83. arXiv: 1510 . 02078. URL: <http://www.vbettadapura.com/egocentric/food/>.
- [35] Timo Ojala, Matti Pietikäinen, and Topi Mäenpää. “Multiresolution gray-scale and rotation invariant texture classification with local binary patterns”. In: *IEEE Transactions on Pattern Analysis and Machine Intelligence* 24.7 (2002), pp. 971–987. ISSN: 01628828. DOI: 10 . 1109/TPAMI . 2002 . 1017623.
- [36] Ming-Kuei Hu. “Visual pattern recognition by moment invariants”. In: *IRE Transactions on Information Theory* 8 (1962), pp. 179–187. ISSN: 0096-1000. DOI: 10 . 1109/TIT . 1962 . 1057692.
- [37] David G Lowe. “Distinctive image features from scale invariant keypoints”. In: *International Journal of Computer Vision* 60.2 (2004), pp. 91–110. ISSN: 0920-5691. DOI: <http://dx.doi.org/10.1023/B:VISI.0000029664.99615.94>. arXiv: 0112017 [cs]. URL: <http://portal.acm.org/citation.cfm?id=996342>.
- [38] Relja Arandjelovic and Andrew Zisserman. “Three things everyone should know to improve object retrieval c”. In: *IEEE Conference on computer vision and Pattern Recognition* April (2012), pp. 2911–2918. ISSN: 9781467312288. DOI: 10 . 1109/CVPR . 2012 . 6248018.
- [39] Herbert Bay, Tinne Tuytelaars, and Luc Van Gool. “SURF: Speeded up robust features”. In: *Lecture Notes in Computer Science (including subseries Lecture Notes in Artificial Intelligence and Lecture Notes in Bioinformatics)*. Vol. 3951 LNCS. 2006, pp. 404–417. ISBN: 3540338322. DOI: 10 . 1007/11744023_32.
- [40] David Arthur and Sergei Vassilvitskii. “k-means++: The Advantages of Careful Seeding”. In: *Proceedings of the eighteenth annual ACM-SIAM symposium on Dis-*

- crete algorithms* 8 (2007), pp. 1027–1035. URL: <http://portal.acm.org/citation.cfm?id=1283494>.
- [41] A Vedaldi and A Zisserman. “Efficient Additive Kernels via Explicit Feature Maps”. In: *{IEEE} Int. Conf. on Computer Vision and Pattern Recognition XX.Xx* (2010), pp. 3539–3546.
- [42] J. Johnson. *CS231n Convolutional Neural Networks for Visual Recognition*. 2016. URL: <http://cs231n.github.io/>.
- [43] Škrjanec Marko. “Automatic fruit recognition using computer vision”. Mentor: Matej Kristan. Bsc thesis. Faculty of Computer and Information Science, University of Ljubljana, 2013.
- [44] Giovanni Maria Farinella, Dario Allegra, and Filippo Stanco. “A benchmark dataset to study the representation of food images”. In: *Lecture Notes in Computer Science (including subseries Lecture Notes in Artificial Intelligence and Lecture Notes in Bioinformatics)* 8927 (2015), pp. 584–599. ISSN: 16113349. DOI: 10.1007/978-3-319-16199-0_41. arXiv: 1410.2488.
- [45] Parisa Pouladzadeh Abdulsalam Yassine and Shervin Shirmohammadi. “FooDD: Food Detection Dataset for Calorie Measurement Using Food Images”. In: *New Trends in Image Analysis and Processing – ICIAP 2015 Workshops* 9281 (2015), pp. 441–448. ISSN: 16113349. DOI: 10.1007/978-3-319-23222-5. URL: http://link.springer.com/chapter/10.1007/978-3-319-23222-5%7B%5C_%7D54.
- [46] Jianming Zhang et al. “Unconstrained Salient Object Detection via Proposal Sub-set Optimization”. In: *IEEE Conference on Computer Vision and Pattern Recognition(CVPR)* (2016). URL: <http://cs-people.bu.edu/jmzhang/sod.html>.

- [47] Karen Simonyan and Andrew Zisserman. “Very Deep Convolutional Networks for Large-Scale Image Recognition”. In: *ImageNet Challenge* (2014), pp. 1–10. ISSN: 09505849. DOI: 10.1016/j.infsof.2008.09.005. arXiv: 1409.1556. URL: <http://arxiv.org/abs/1409.1556>.
- [48] Travis E Oliphant. “SciPy: Open source scientific tools for Python”. In: *Computing in Science and Engineering* 9 (2007), pp. 10–20. ISSN: 1521-9615. URL: <http://www.scipy.org/>.
- [49] Stéfan Van Der Walt, S. Chris Colbert, and Gaël Varoquaux. “The NumPy array: A structure for efficient numerical computation”. In: *Computing in Science and Engineering* 13.2 (2011), pp. 22–30. ISSN: 15219615. DOI: 10.1109/MCSE.2011.37. arXiv: 1102.1523.
- [50] Wes McKinney. “Data Structures for Statistical Computing in Python”. In: *Proceedings of the 9th Python in Science Conference* (2010), pp. 51–56. URL: <http://conference.scipy.org/proceedings/scipy2010/mckinney.html>.
- [51] Stéfan van der Walt et al. “Scikit-image: image processing in Python”. In: *PeerJ* 2 (2014), e453. ISSN: 2167-8359. DOI: 10.7717/peerj.453. arXiv: 1407.6245. URL: <https://peerj.com/articles/453>.
- [52] G Bradski. “The OpenCV Library”. In: *Dr Dobbs Journal of Software Tools* 25 (2000), pp. 120–125. ISSN: 1044-789X. DOI: 10.1111/0023-8333.50.s1.10. URL: <http://opencv.org/>.
- [53] Fabian Pedregosa et al. “Scikit-learn: Machine Learning in Python”. In: *... of Machine Learning ...* 12 (2012), pp. 2825–2830. ISSN: 15324435. DOI: 10.1007/s13398-014-0173-7.2. arXiv: 1201.0490. URL: <http://scikit-learn.org/stable/>.

- [54] Yangqing Jia et al. “Caffe: Convolutional Architecture for Fast Feature Embedding”. In: *Proceedings of the ACM International Conference on Multimedia* (2014), pp. 675–678. ISSN: 10636919. DOI: 10.1145/2647868.2654889. arXiv: 1408.5093. URL: <http://arxiv.org/abs/1408.5093>.
- [55] John D. Hunter. “Matplotlib: A 2D graphics environment”. In: *Computing in Science and Engineering* 9.3 (2007), pp. 99–104. ISSN: 15219615. DOI: 10.1109/MCSE.2007.55.
- [56] M. Everingham et al. *The PASCAL Visual Object Classes Challenge 2012 (VOC2012) Results*. URL: <http://www.pascal-network.org/challenges/VOC/voc2012/workshop/index.html>.